LIGO-G1601021

RESULTS OF SEARCHING FOR BINARY BLACK HOLES IN THE FIRST OBSERVING RUN OF ADVANCED LIGO

Collin Capano

Max Planck Institute for Gravitational Physics

Hannover, Germany

on behalf of the LIGO Scientific Collaboration and the Virgo Collaboration

GR21, New York

- First observing run of Advanced LIGO (O1) occurred 12 September, 2015 – 19 January, 2016
- 2 confident detections made:
  - GW150914 ("The Event"): 14 Sept. 2015 at 09:50:45 UTC [1]
  - GW151226 ("Boxing day Event"): 26 Dec 2015 03:38:53 UTC [2]
  - Both > 5.3σ [3]
- Third possible signal detected with lower significance, LVT151012 [1]
  - 87% chance that is astrophysical in origin [3]

1. LSC+Virgo , PRL 116, 061102 (2016)
2. LSC+Virgo, PRL 116, 241103 (2016)
3. LSC+Virgo, arXiv:1606.04856

1. Search description & results
2. Parameter estimation of events
3. Testing GR with observations
4. Looking forward

1. SEARCH DESCRIPTION & RESULTS

TWO MODELED SEARCHES PERFORMED

- PyCBC [4]
  - Python based, frequency-domain matched filter workflow to compute signal-to-noise ratio (SNR)
  - Uses a chi-squared statistic to re-weight SNR
  - Analyzed 46.1 days of coincident data
- GstLAL [5]
  - gStreamer based, time-domain matched filter workflow
  - implements a different ranking statistic from PyCBC
  - Analyzed 48.3 days of coincident data

4. S. A. Usman et al., arXiv:1508.02357
5. C. Messick et al., arXiv:1604.04324

THE BANK USED IN O1

- 4 free parameters
  - 2 component masses
  - 2 (non-precessing) spins
- We limit NS spin to $|\chi_{NS}| < 0.05$
- Is sensitive to NS with $|\chi_{NS}| < 0.4$ [6]
- Assume BHs can have $m \geq 2\ M_\odot$
- $|\chi_{BH}| < 0.9895$

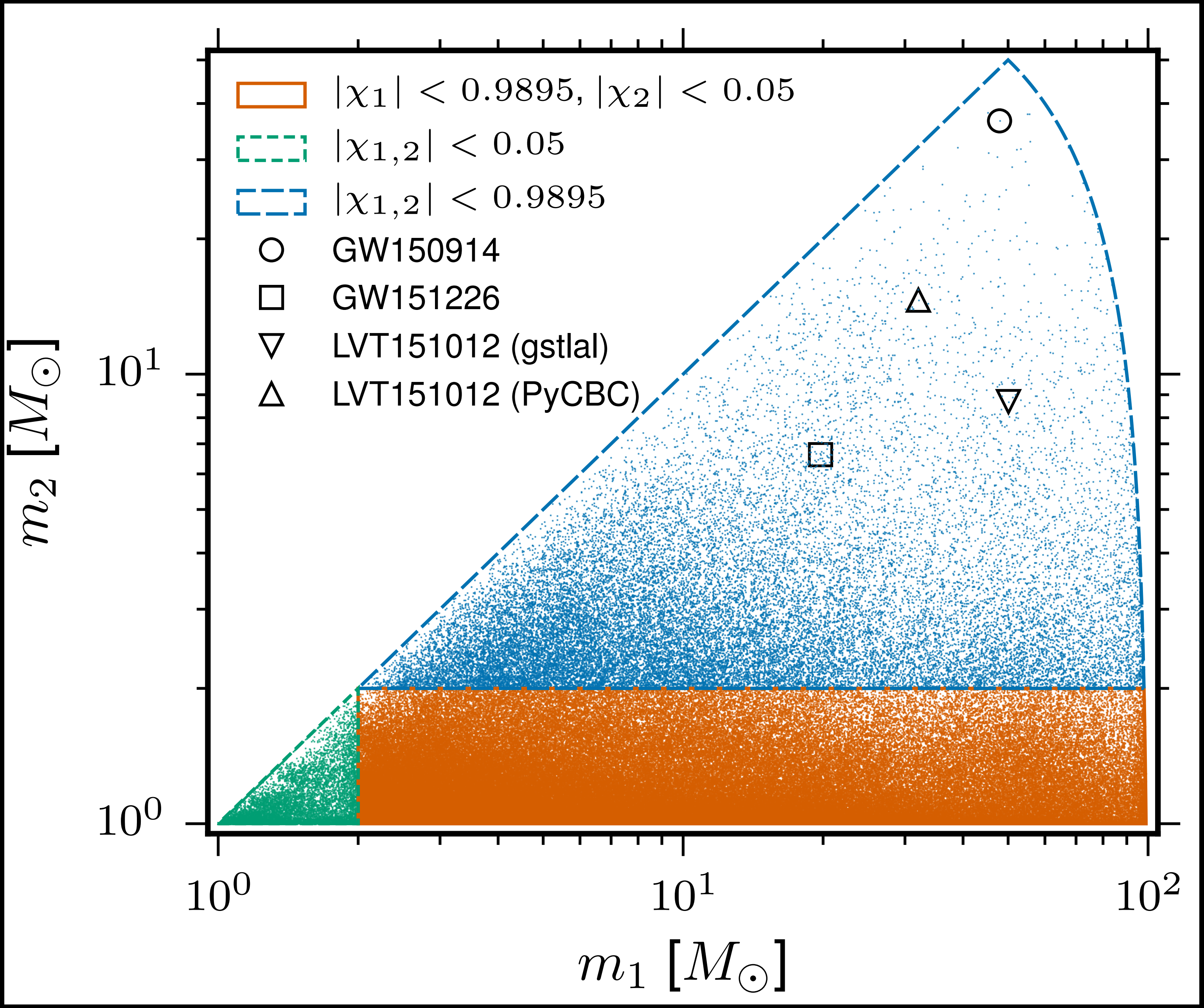

LSC+Virgo, arXiv:1606.04856

6. A. Nitz, Ph.D. thesis (2015)

IN A NUTSHELL

- Filter each template with data to obtain *triggers*
- Enforce coincidence to obtain *events*: triggers must occur in same template within +/-15ms at each detector
- Compute ranking statistic for events, select template with largest ranking statistic
- Repeat with data shifted in time between detectors to obtain rate of *background* chance events

FIRST 16 DAYS

PyCBC

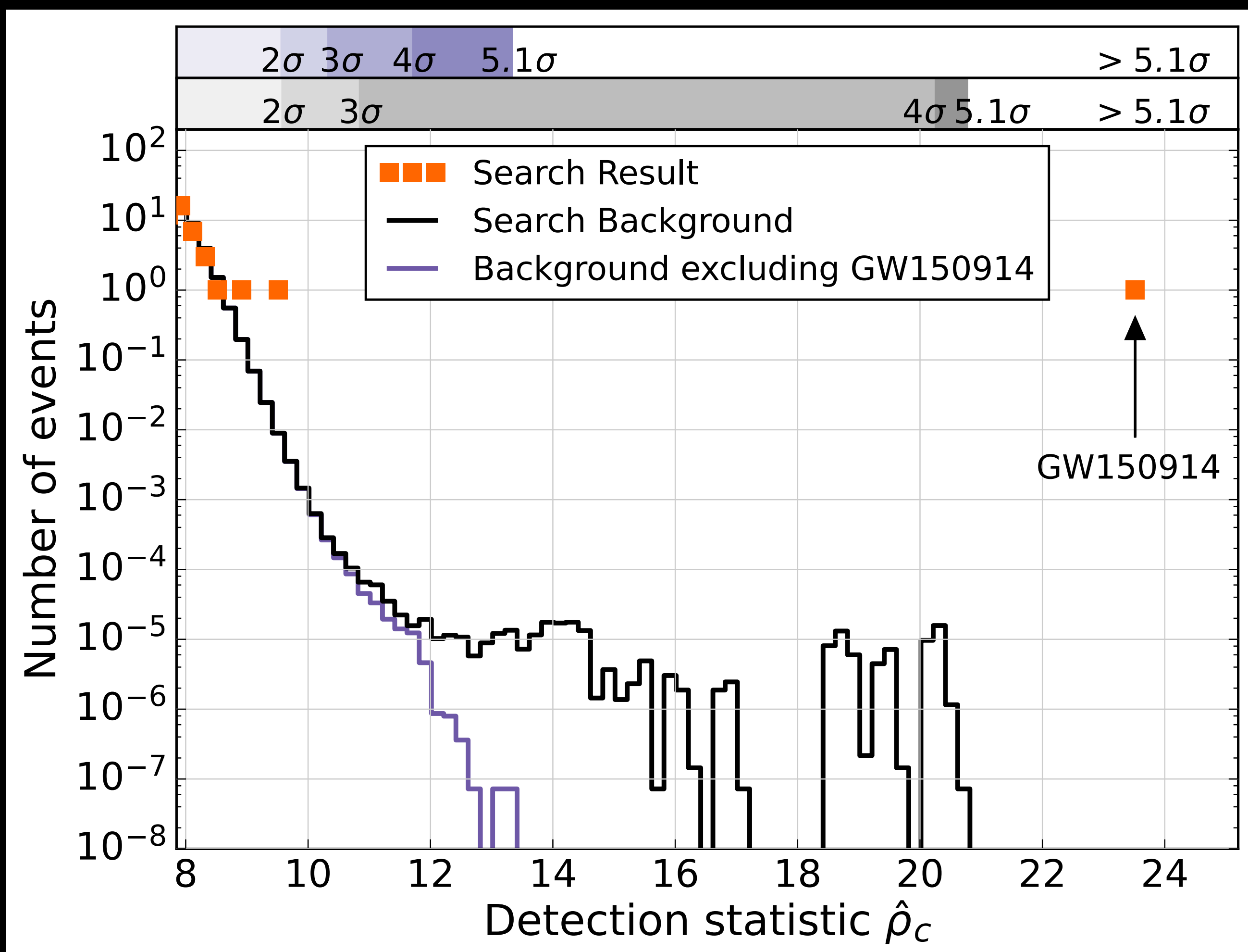

GstLAL

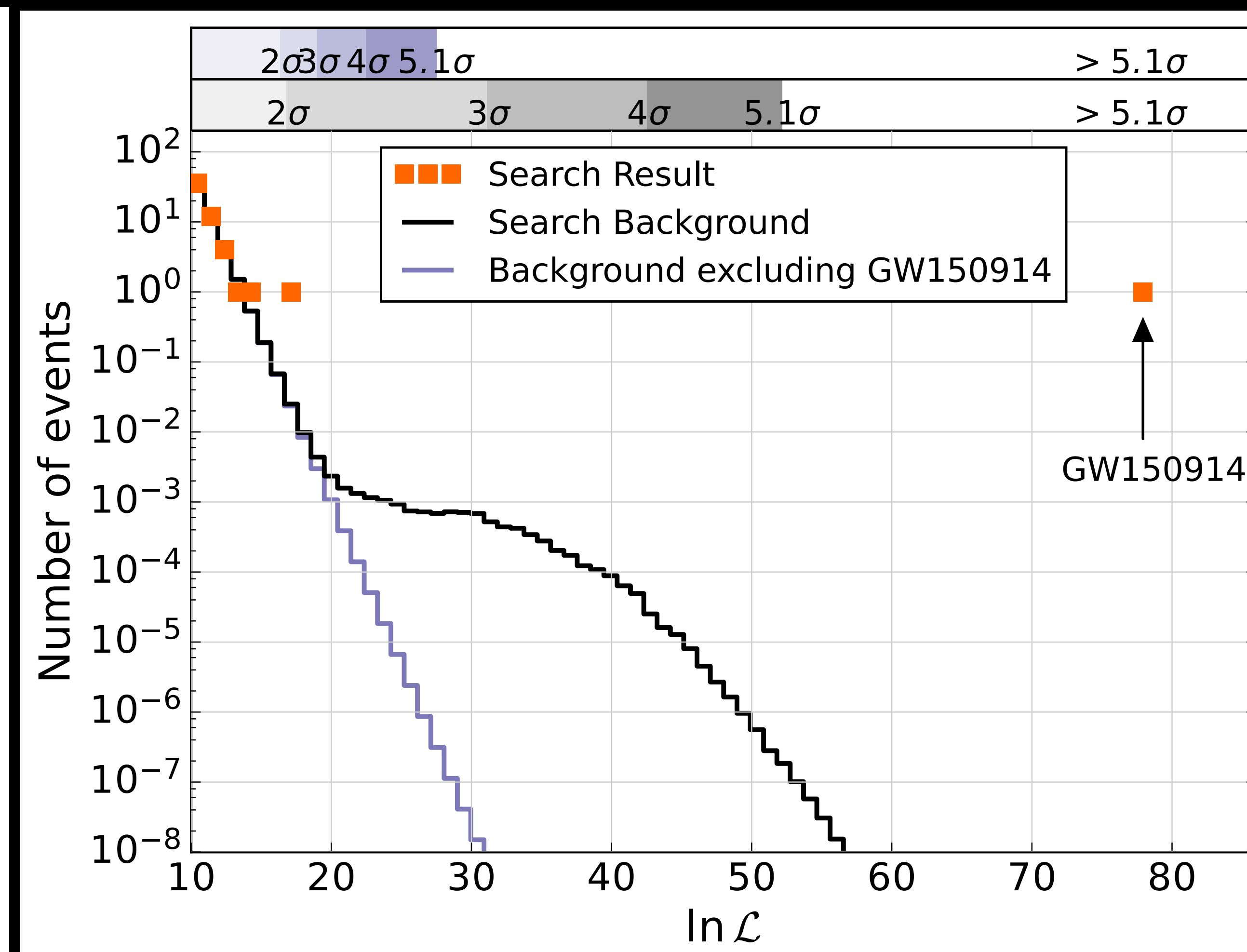

LSC+Virgo, PRD 93, 122003 (2016)

GW150914

- Initially reported using first 16 days of O1 coincident data [7,8]
- Louder than all background
- FAR < 5 x 10^{-6}/ year
- p-value < 2 x 10^{-7} (> 5.1σ)

8. LSC+Virgo, PRL 116, 061102 (2016)
9. LSC+Virgo, PRD 93, 122003 (2016)

O1

PyCBC

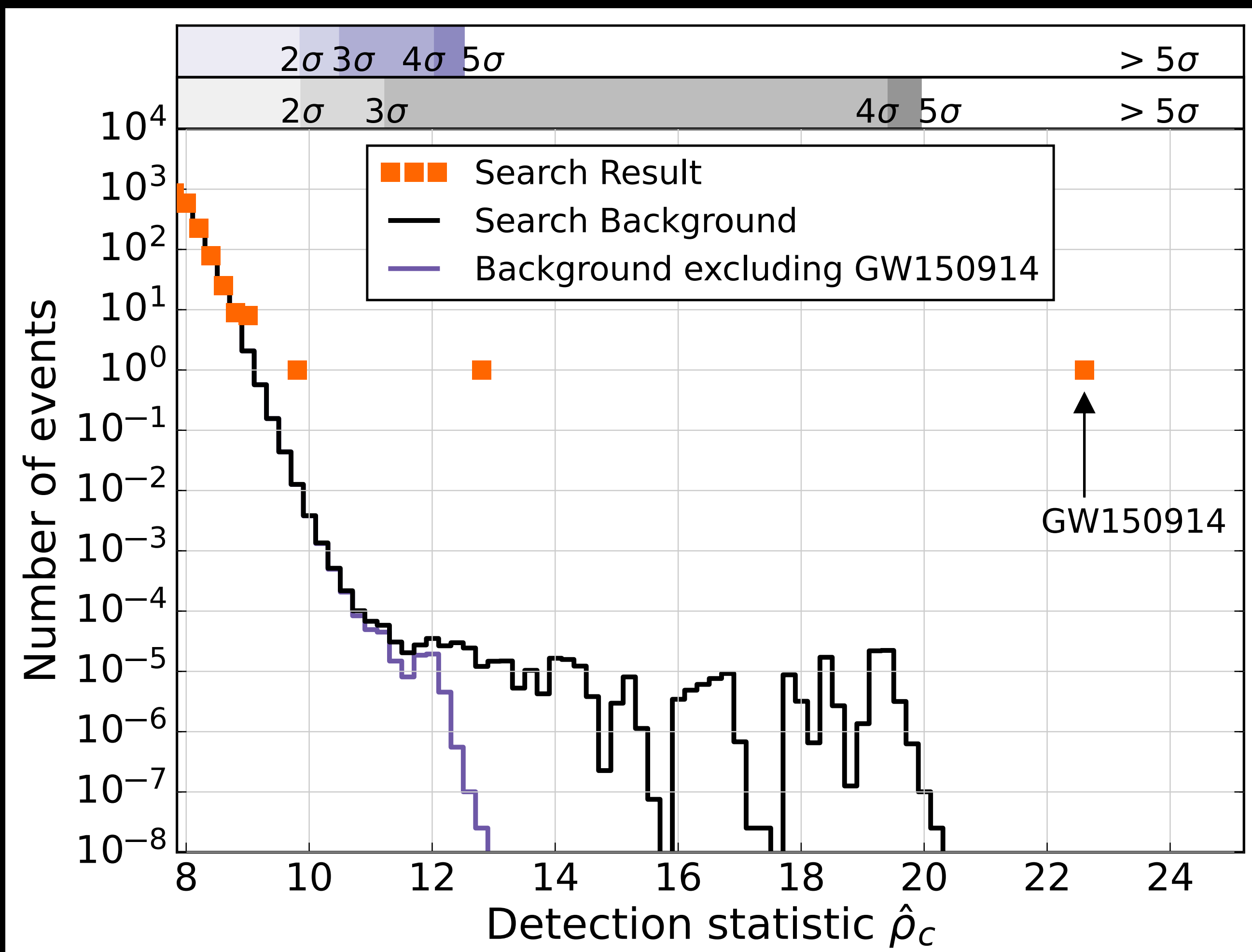

GstLAL

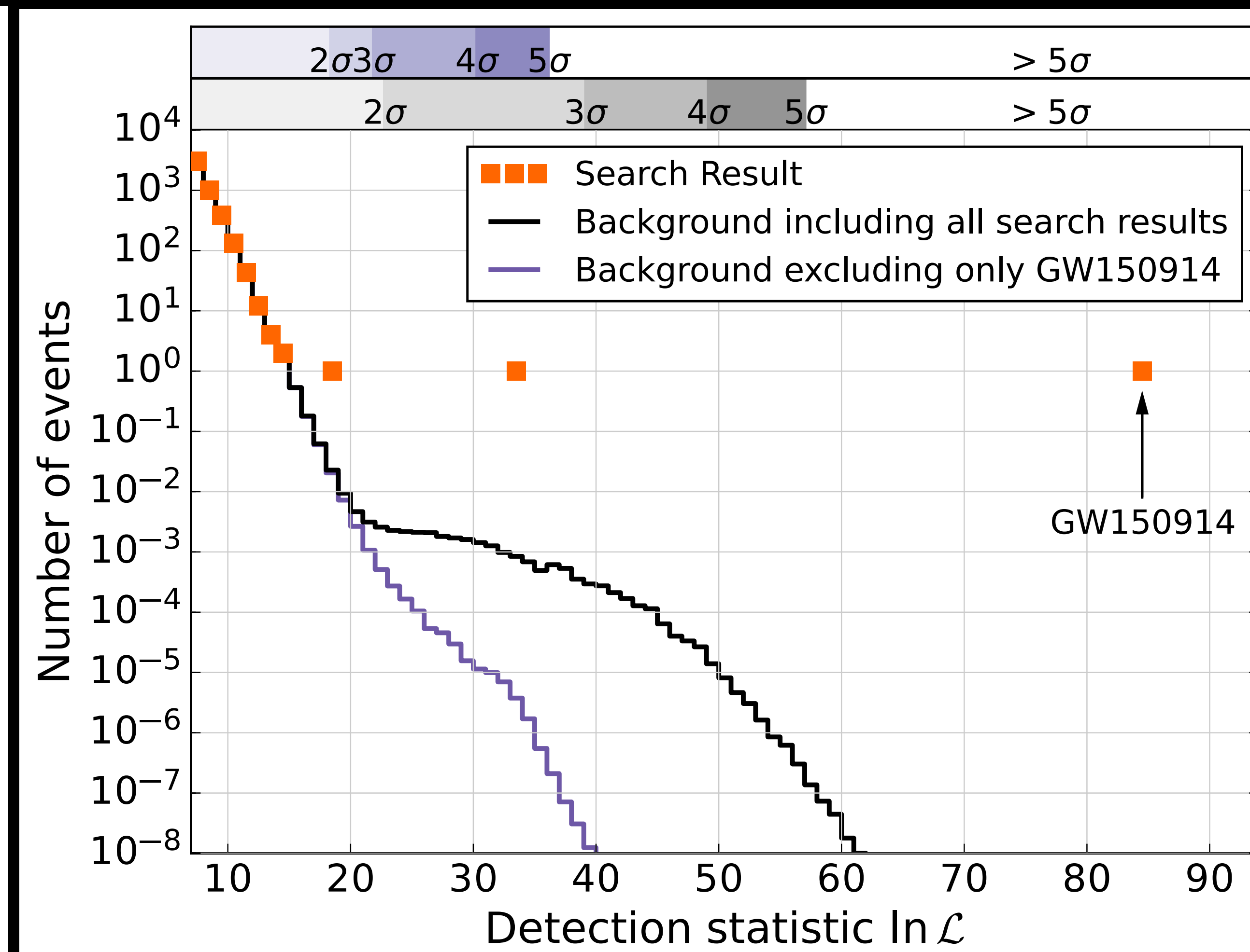

LSC+Virgo, arXiv:1606.04856

GW150914

- Use all of O1 to estimate background
- Still louder than all background
- FAR < 6 x 10^{-7} / year
- p-value < 6 x 10^{-8} (> 5.3σ)

O1 - GW150914

PyCBC

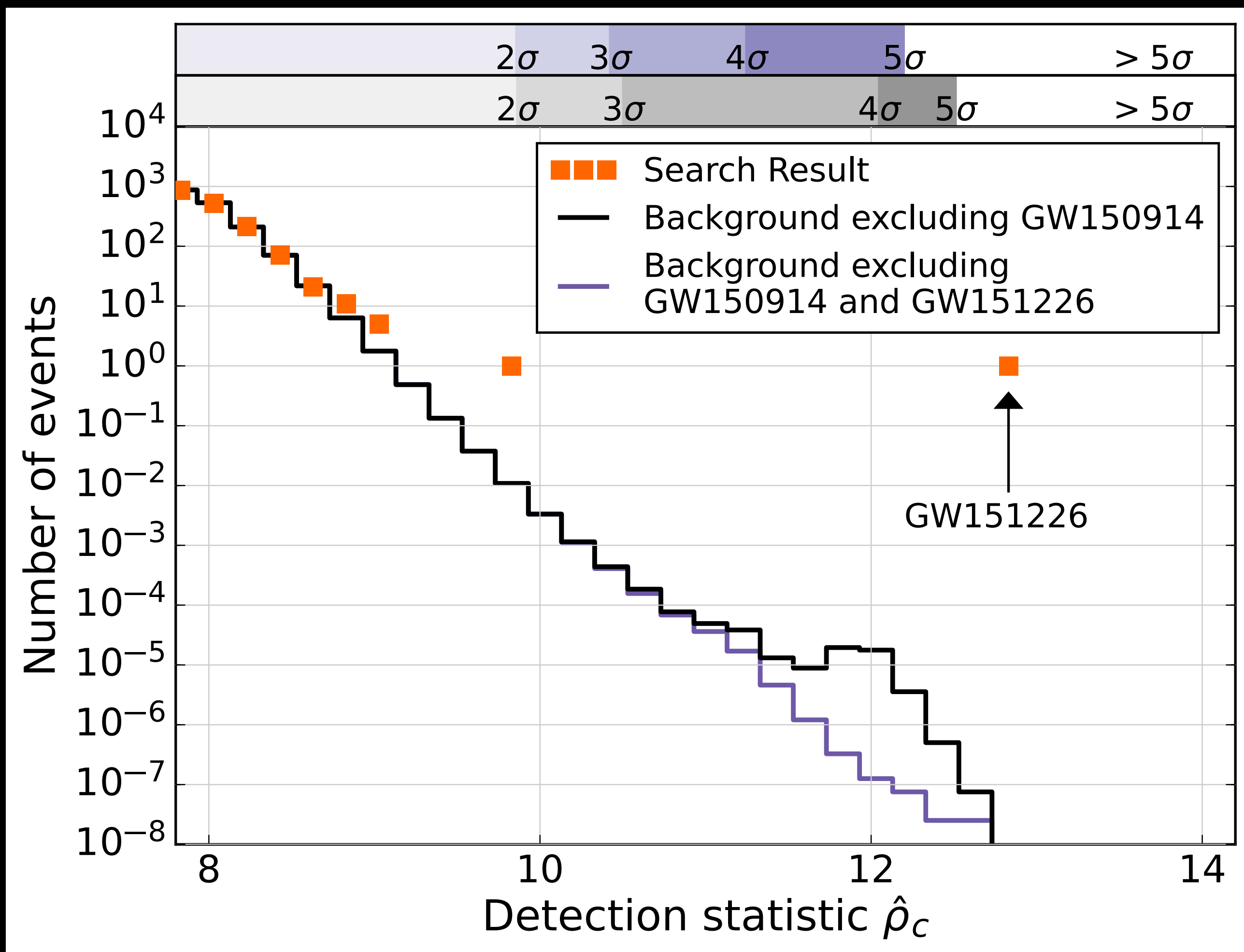

GstLAL

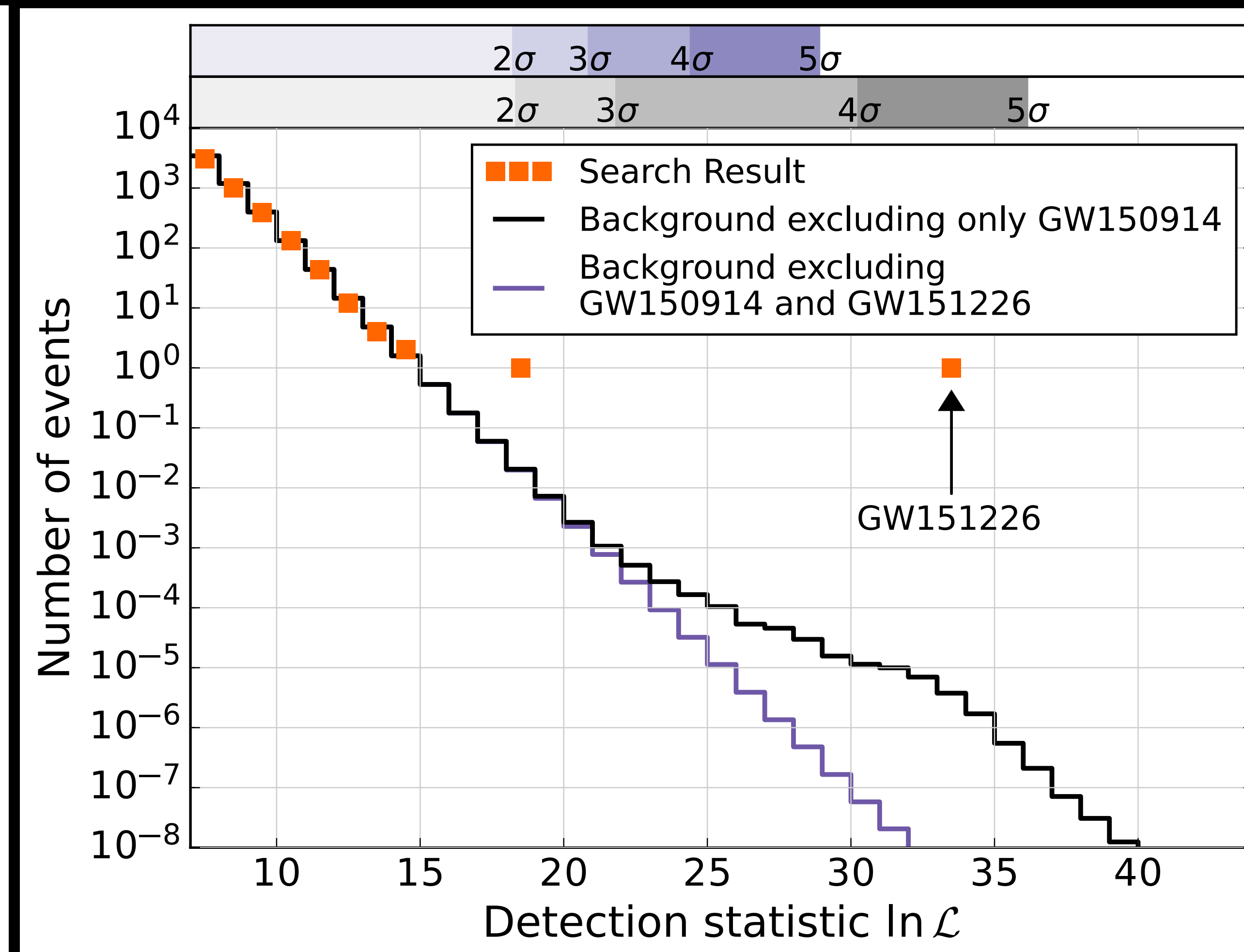

LSC+Virgo, arXiv:1606.04856

GW151226

- PyCBC: Louder than all background when GW150914 is removed
  - FAR < 6 x 10^{-7} / year
  - p-value < 6 x 10^{-8} (> 5.3σ)
- GstLAL:
  - FAR = 2 x 10^{-7} / year
  - p-value = 3.5 x 10^{-8} (4.5σ)

O1 - GW150914

PyCBC

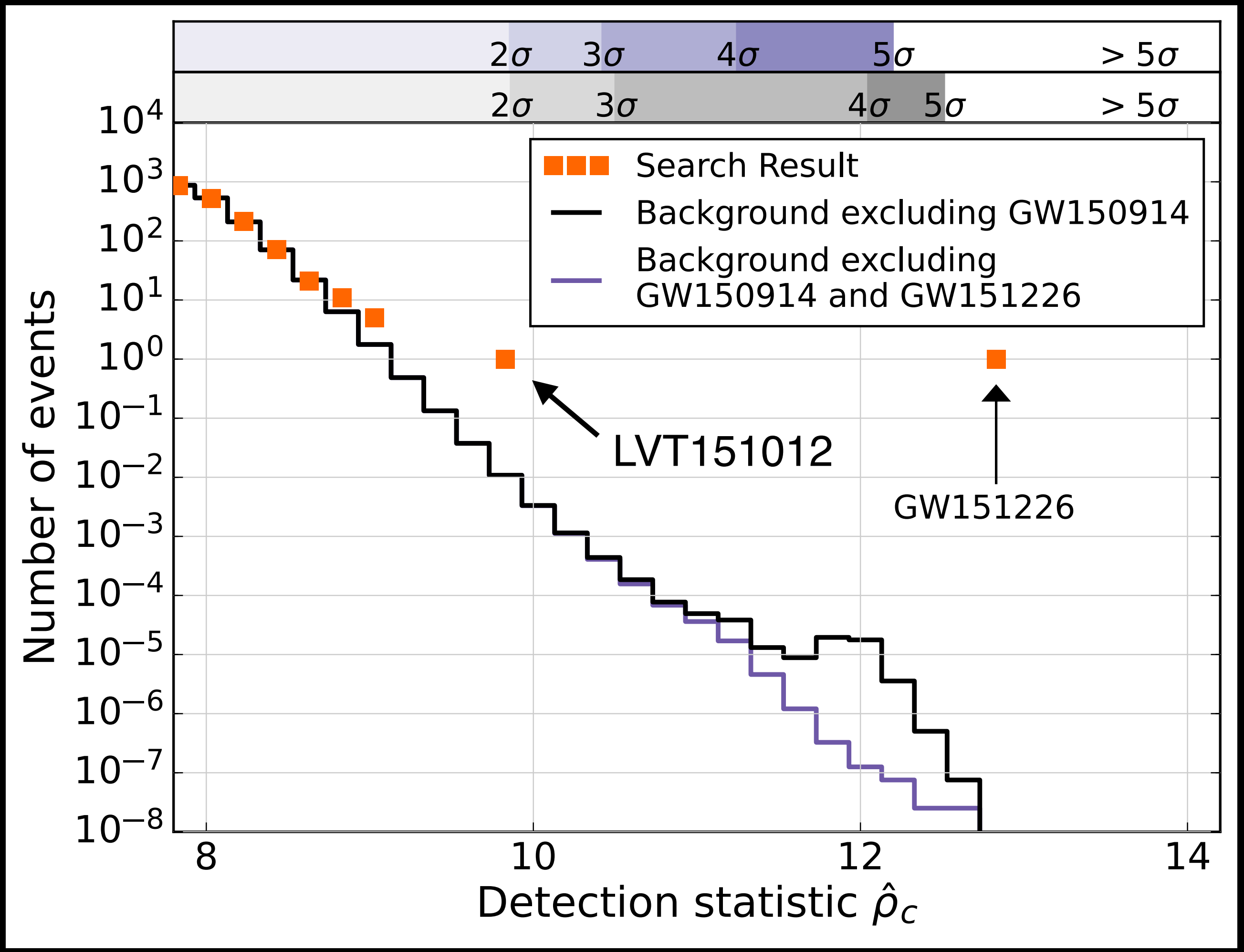

GstLAL

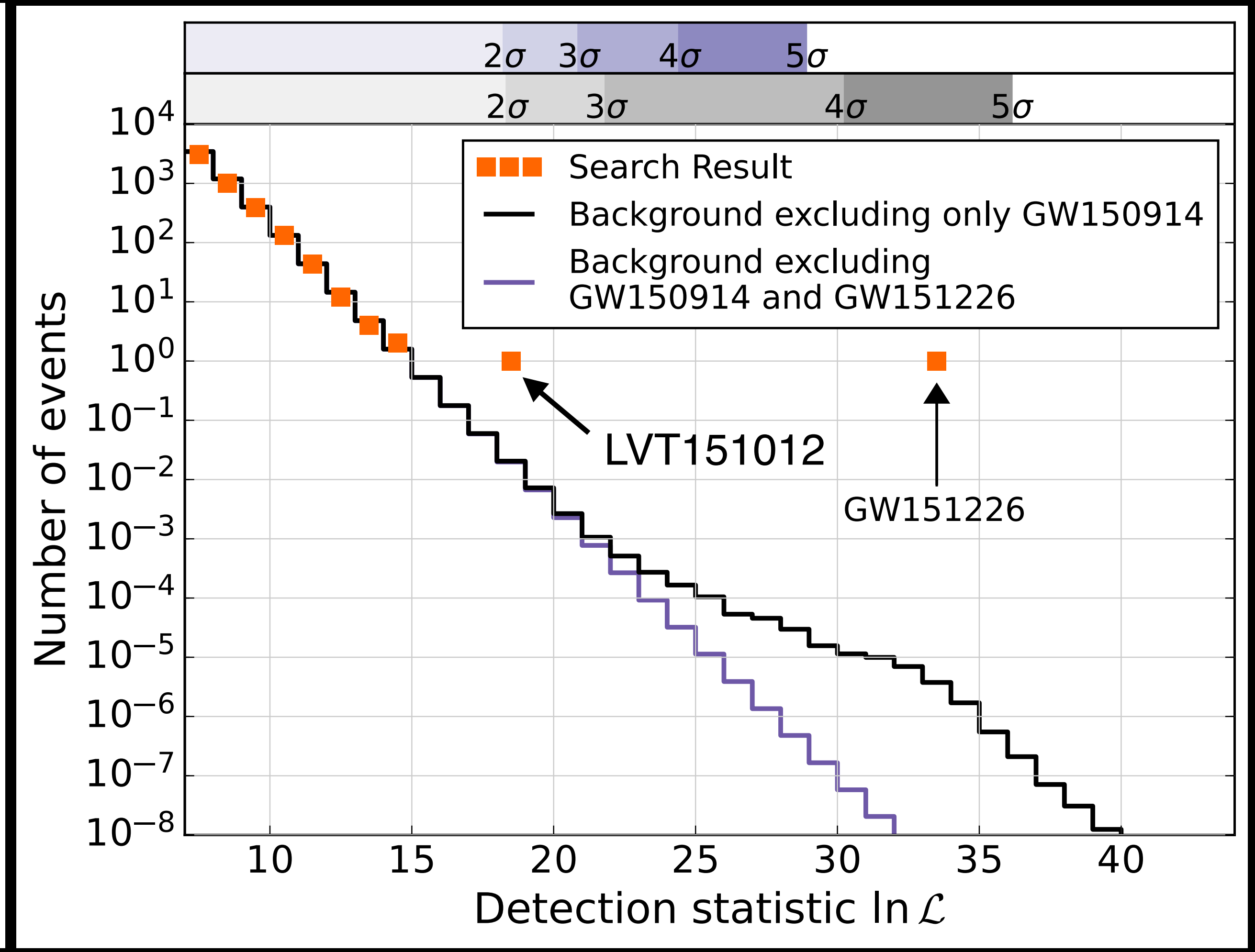

LSC+Virgo, arXiv:1606.04856

LVT151012

- PyCBC: FAR = 1/2.7 years (1.7σ)
- GstLAL: FAR = 1/5.9 years (2.0σ)
- Not significant enough to claim as definitive event
- *However…* parameters consistent with population of BBH signals
- Based on rate estimate of BBHs, 87% probability that it is a signal

3. PARAMETER ESTIMATION

MCMC & Nested Sampling

- Use 2 independent stochastic sampling engines to evaluate likelihood over multi-dimensional parameter space
  - Markov-chain Monte Carlo (MCMC) [9,10]
  - Nested sampling [11,12]
- Time and mass estimate from searches used to inform prior
  - t_c: +/-0.1s uniform prior centered on searches' t_c

9. C. Rover et al., CQG 23, 4895 (2006)
10. M. van der Sluys et al., CQG 25, 184011(2008)
11. J. Skilling, Bayesian Analysis 1, 833 (2006)
12. J. Veitch & A. Vecchio, PRD 81, 062003 (2010)

Luminosity distance

- GW150914:

$$D_{\mathrm{L}} = 420^{+150}_{-180}\,\mathrm{Mpc}$$

- GW151226:

$$D_{\mathrm{L}} = 440^{+180}_{-190}\,\mathrm{Mpc}$$

- LVT151012:

$$D_{\mathrm{L}} = 1000^{+500}_{-500}\,\mathrm{Mpc}$$

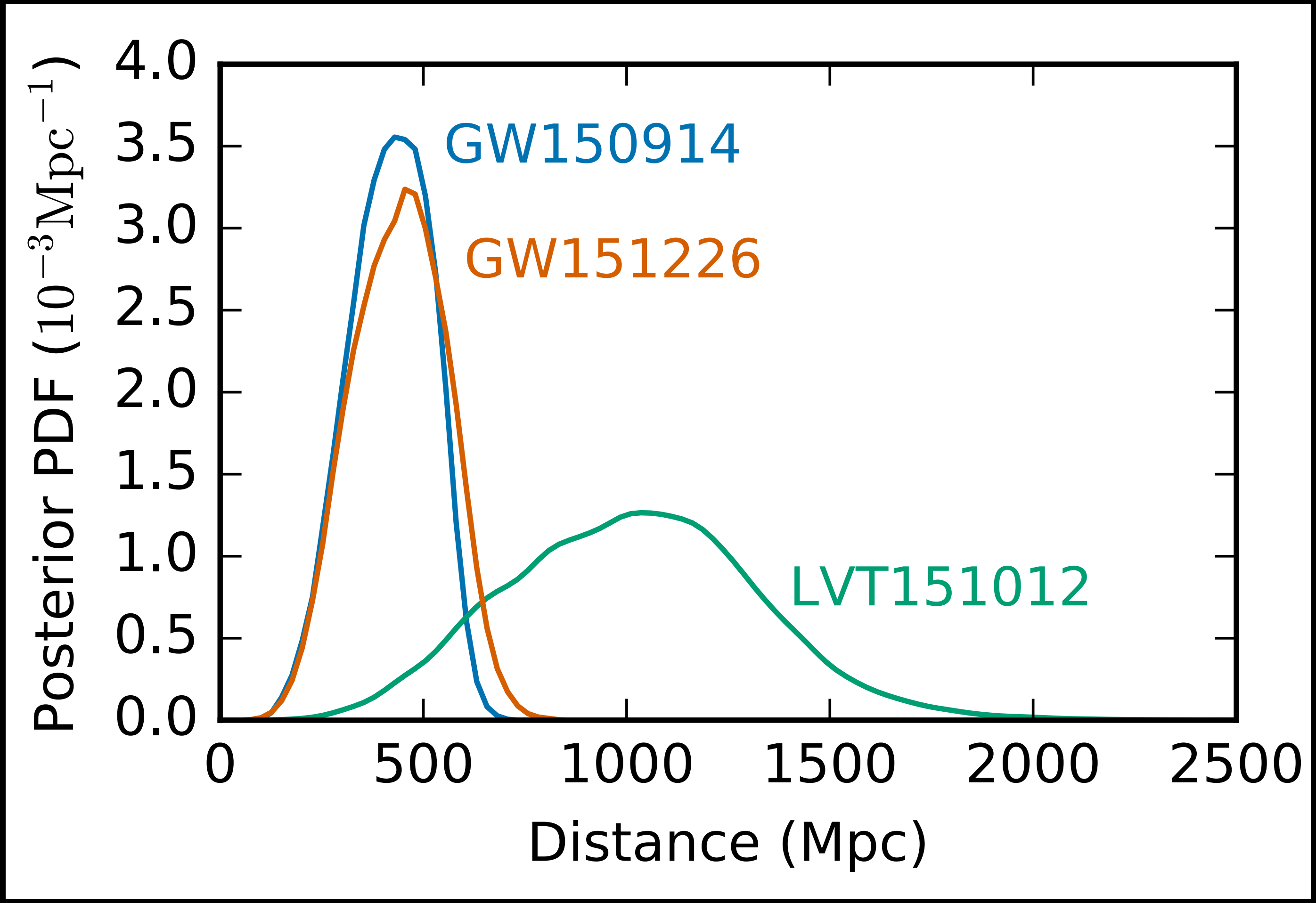

LSC+Virgo, arXiv:1606.04856

Luminosity distance

- GW150914:

$$D_\mathrm{L} = 420^{+150}_{-180}\,\mathrm{Mpc}$$
$$z = 0.09^{+0.03}_{-0.04}$$

- GW151226:

$$D_\mathrm{L} = 440^{+180}_{-190}\,\mathrm{Mpc}$$
$$z = 0.09^{+0.03}_{-0.04}$$

- LVT151012:

$$D_\mathrm{L} = 1000^{+500}_{-500}\,\mathrm{Mpc}$$
$$z = 0.20^{+0.09}_{-0.09}$$

Redshift coupled to masses. We estimate z assuming flat ΛCDM cosmology.*

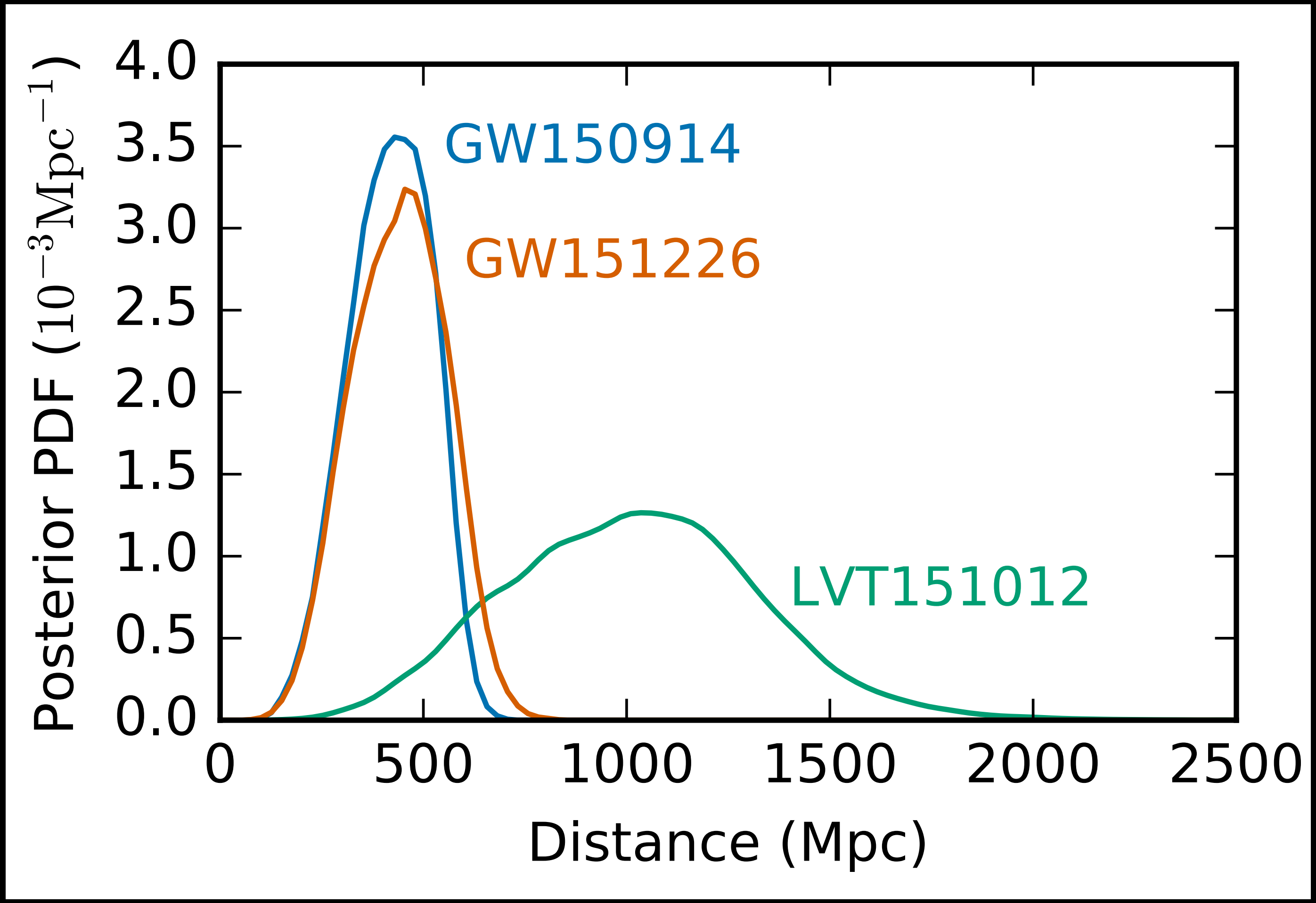

LSC+Virgo, arXiv:1606.04856

$^*H_0 = 67.9\,\mathrm{km\,s^{-1}\,Mpc^{-1}}$

$\Omega_\mathrm{m} = 0.306$

Component masses

- GW150914:

$$m_1^{\text{source}} = 36.2^{+5.2}_{-3.8}\,\mathrm{M}_\odot$$
$$m_2^{\text{source}} = 29.1^{+3.7}_{-4.4}\,\mathrm{M}_\odot$$

- GW151226:

$$m_1^{\text{source}} = 14.2^{+8.3}_{-3.7}\,\mathrm{M}_\odot$$
$$m_2^{\text{source}} = 7.5^{+2.3}_{-2.3}\,\mathrm{M}_\odot$$

- LVT151012:

$$m_1^{\text{source}} = 23^{+18}_{-6}\,\mathrm{M}_\odot$$
$$m_2^{\text{source}} = 13^{+4}_{-5}\,\mathrm{M}_\odot$$

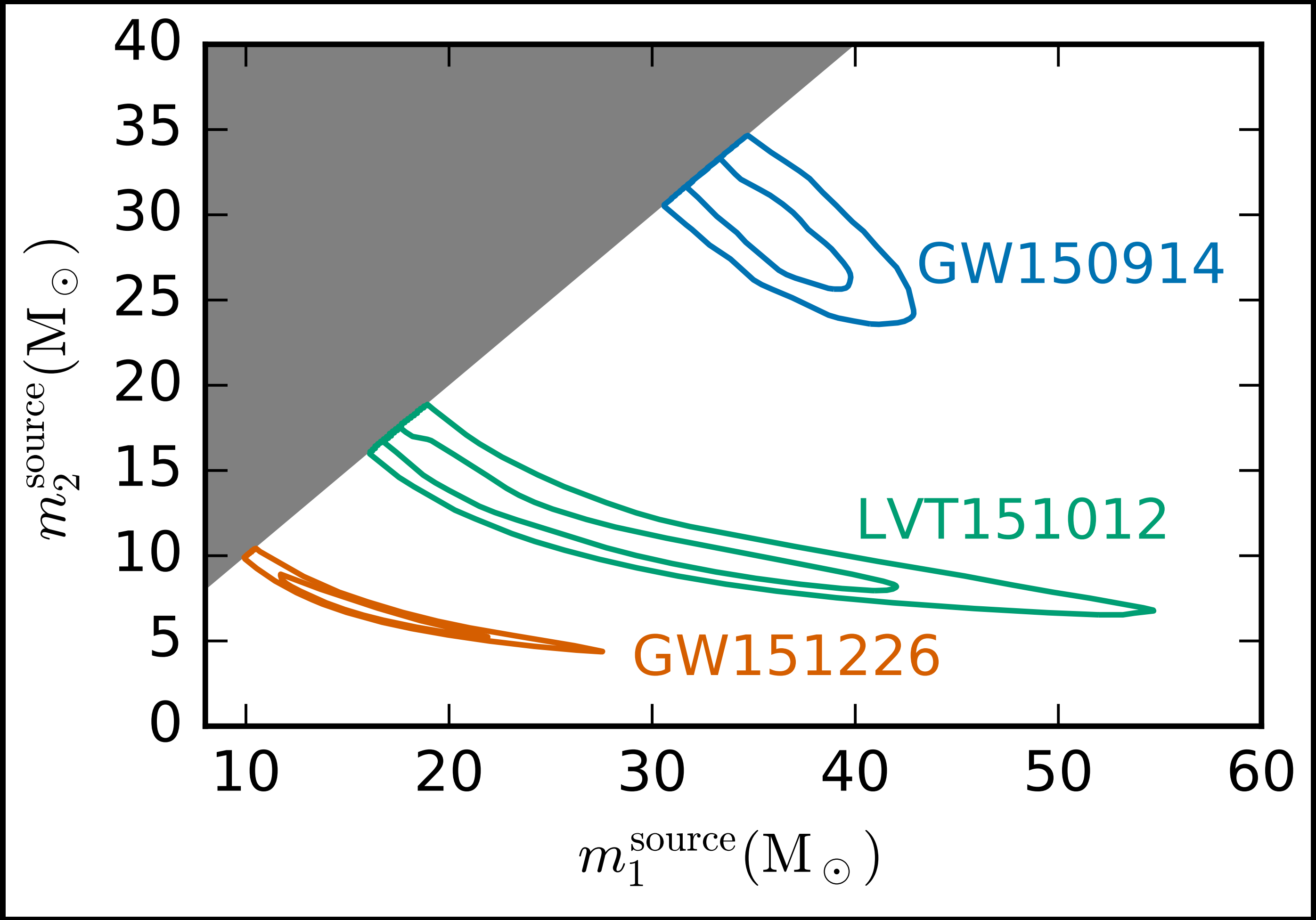

LSC+Virgo, arXiv:1606.04856

COMPONENT MASSES

- GW150914:

$$m_1^{\text{source}} = 36.2^{+5.2}_{-3.8}\,\mathrm{M}_\odot$$
$$m_2^{\text{source}} = 29.1^{+3.7}_{-4.4}\,\mathrm{M}_\odot$$

- GW151226:

$$m_1^{\text{source}} = 14.2^{+8.3}_{-3.7}\,\mathrm{M}_\odot$$
$$m_2^{\text{source}} = 7.5^{+2.3}_{-2.3}\,\mathrm{M}_\odot$$

- LVT151012:

$$m_1^{\text{source}} = 23^{+18}_{-6}\,\mathrm{M}_\odot$$
$$m_2^{\text{source}} = 13^{+4}_{-5}\,\mathrm{M}_\odot$$

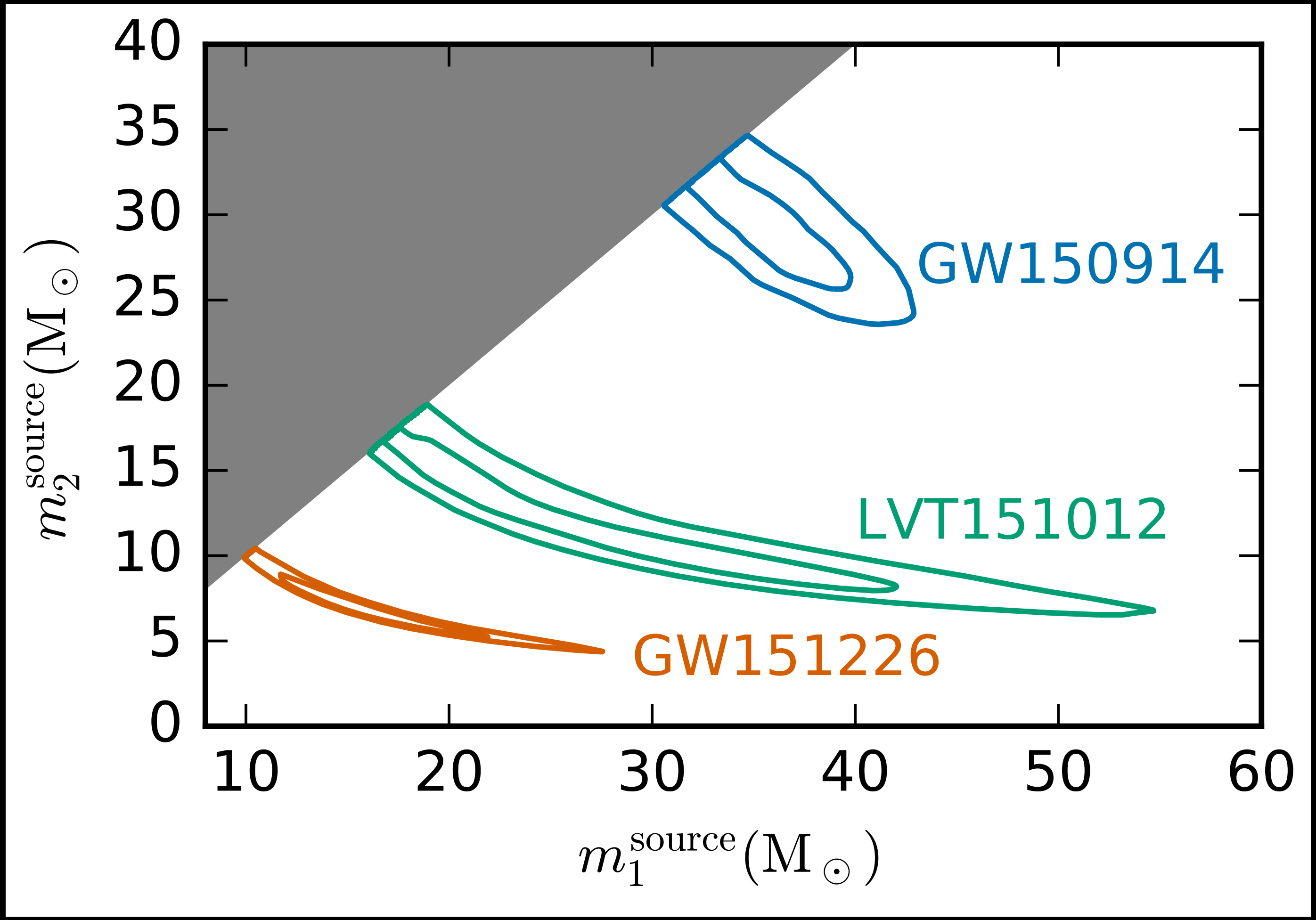

LSC+Virgo, arXiv:1606.04856

None of the components are neutron stars.

Measuring spins

- Individual component spins not well constrained
- Dominant spin effect:

$$\chi_{\rm eff} = \left[\frac{m_1\vec{\chi}_1 + m_2\vec{\chi}_2}{m_1 + m_2}\right] \cdot \hat{\mathbf{L}}$$

- Effective precession parameter:

$$\chi_{\rm p} = \max\left[\chi_{1\perp}, \quad \frac{4q+3}{3q+4} q\chi_{2\perp}\right]; \quad q = m_2/m_1$$

EFFECTIVE SPIN & MASS RATIO

- GW150914:

$$\chi_{\mathrm{eff}} = -0.06^{+0.14}_{-0.14}$$
$$q = 0.81^{+0.19}_{-0.24}$$

- GW151226:

$$\chi_{\mathrm{eff}} = 0.21^{+0.20}_{-0.10}$$
$$q = 0.52^{+0.43}_{-0.33}$$

- LVT151012:

$$\chi_{\mathrm{eff}} = 0.21^{+0.20}_{-0.10}$$
$$q = 0.57^{+0.39}_{-0.41}$$

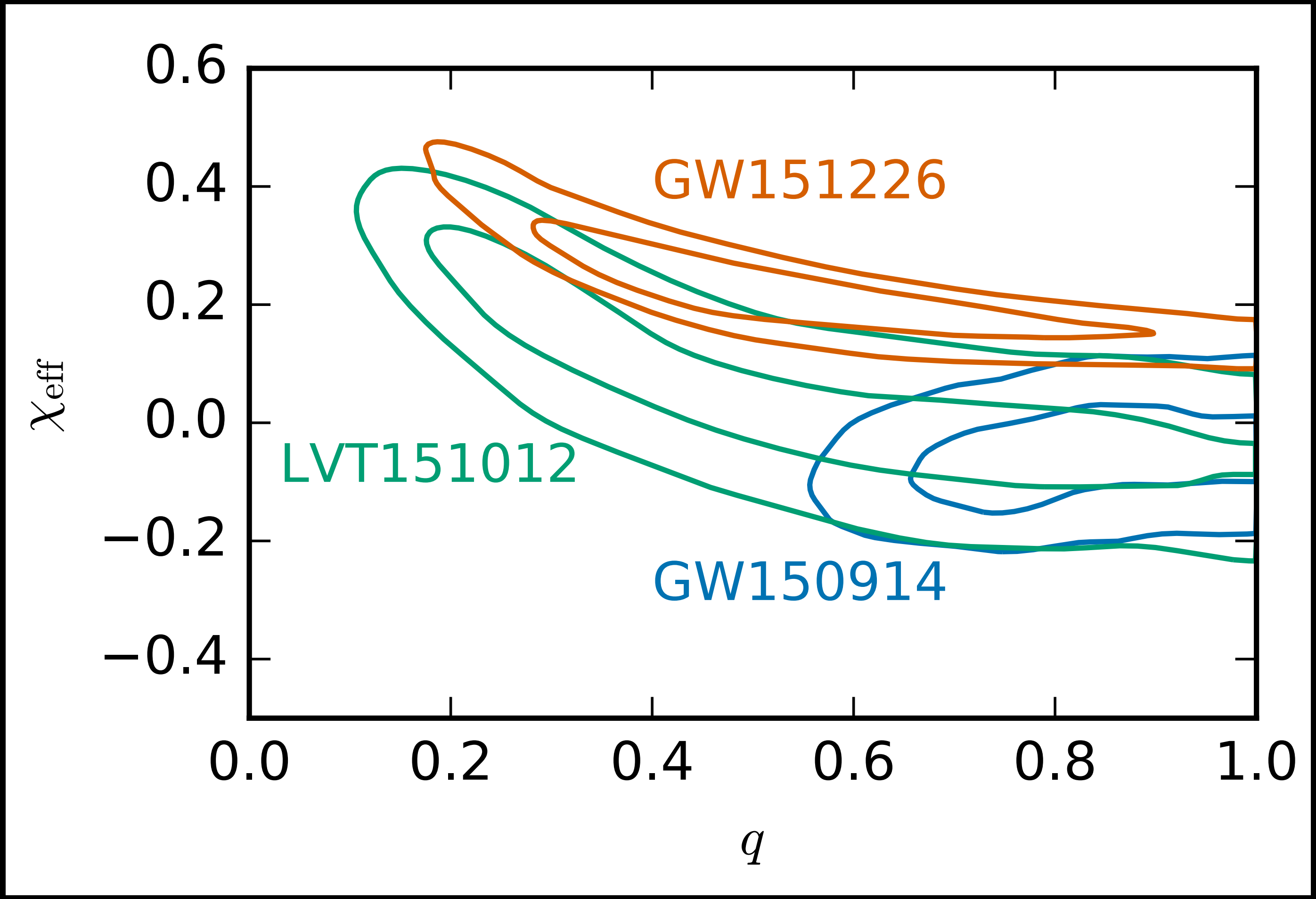

LSC+Virgo, arXiv:1606.04856

GW151226: At least one component has a spin ≥ 0.2. (99% credible level)

PRECESSION: GW150914

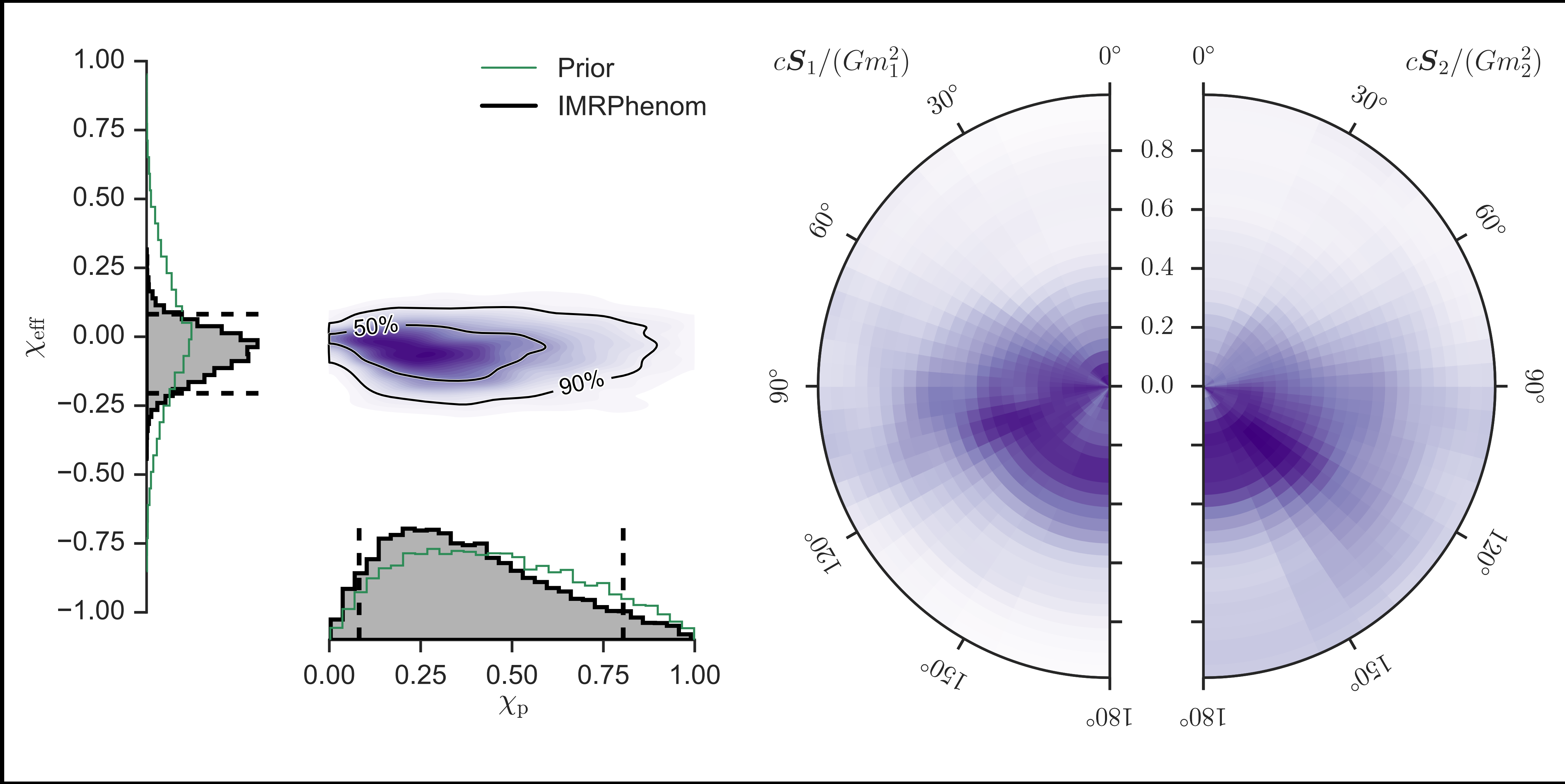

LSC+Virgo, PRL 116, 241102 (2016)

PRECESSION: GW150914

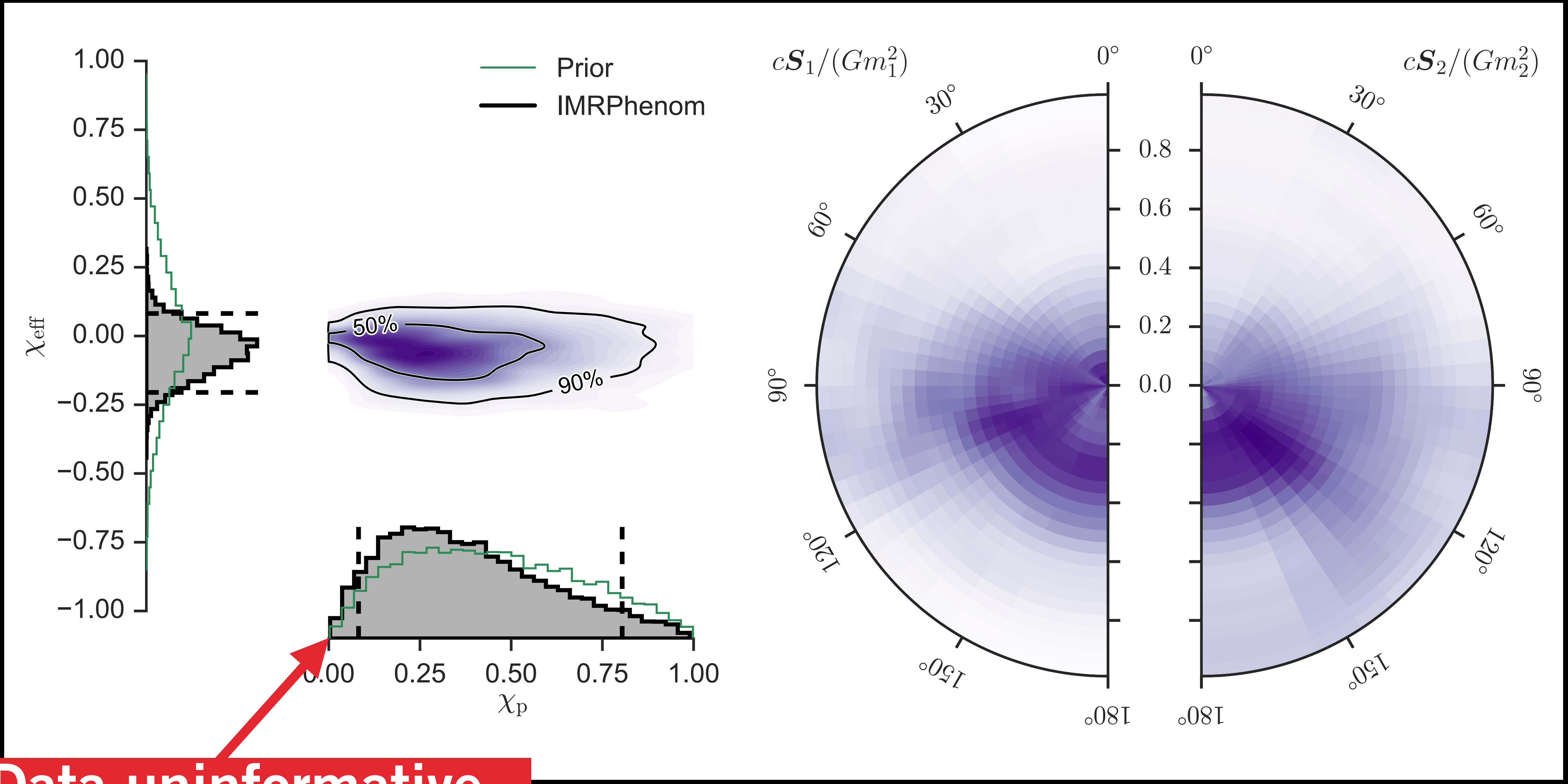

Data uninformative about prcession

LSC+Virgo, PRL 116, 241102 (2016)

PRECESSION: GW151226

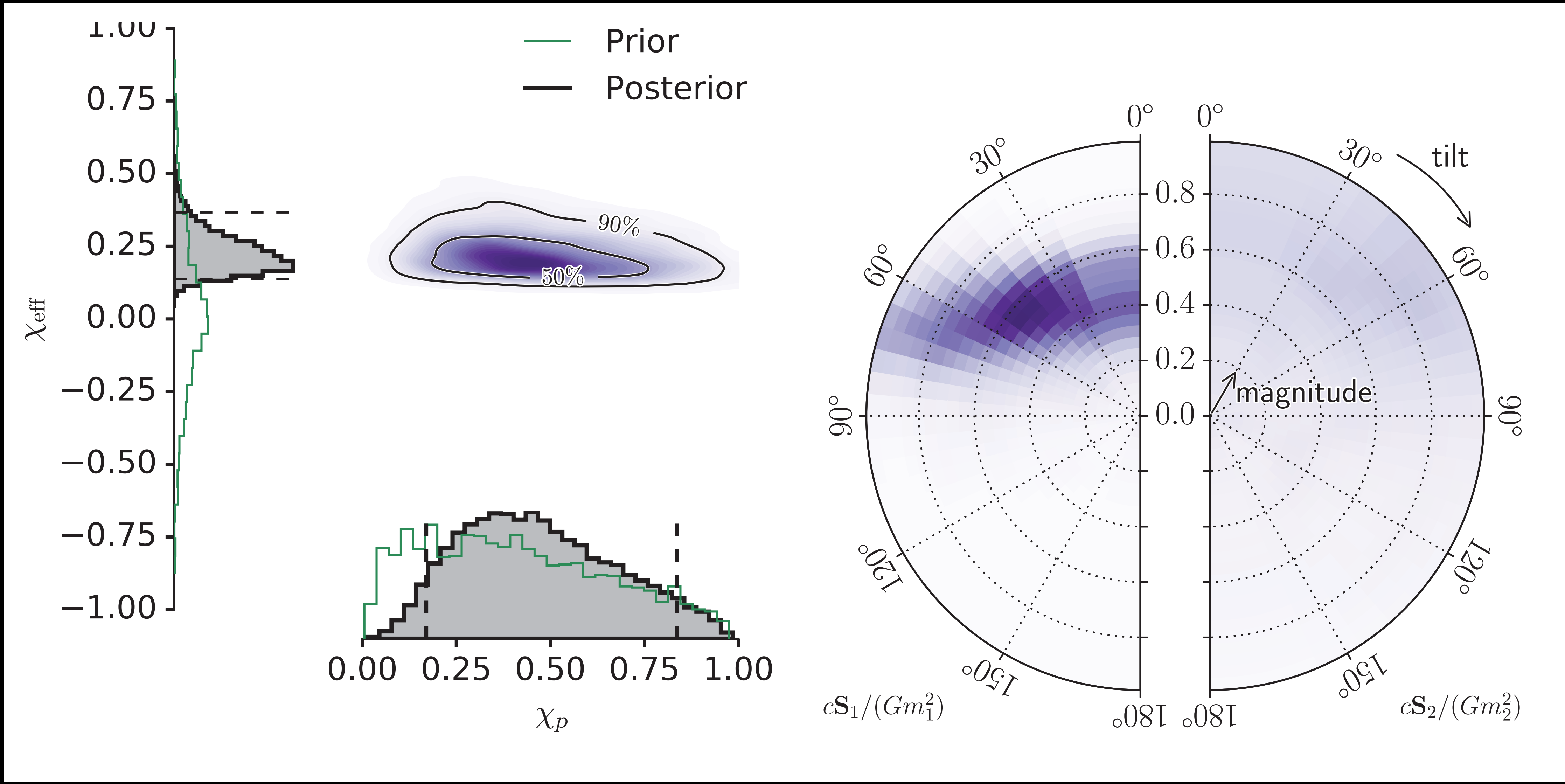

LSC+Virgo, PRL 116, 241103 (2016)

PRECESSION: GW151226

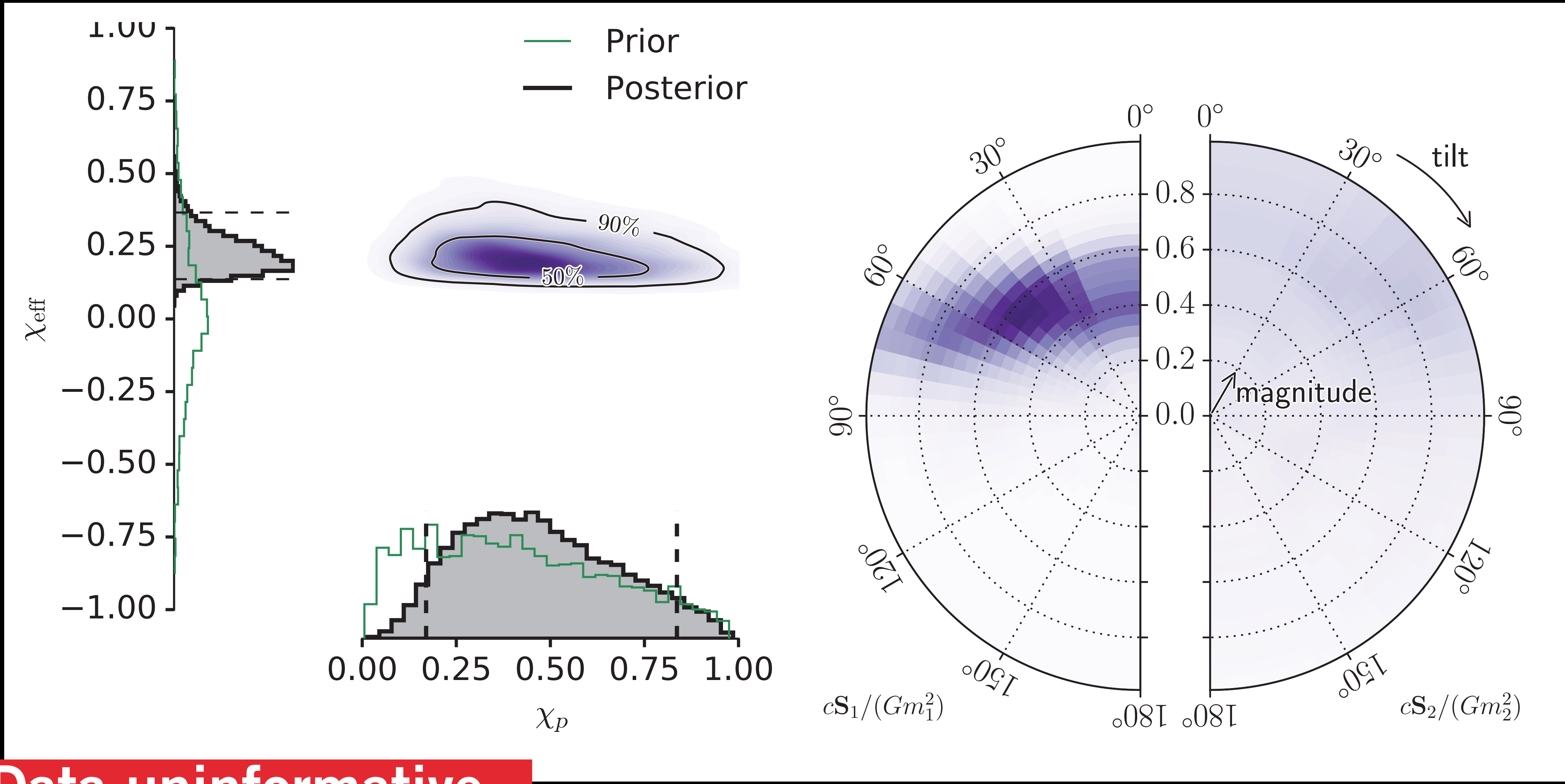

Data uninformative about prcession

LSC+Virgo, PRL 116, 241103 (2016)

Final Mass & Spin*

- GW150914:

$$M_{\rm f}^{\rm source} = 62.3^{+3.7}_{-3.1}\,{\rm M}_\odot$$
$$a_{\rm f} = 0.68^{+0.05}_{-0.06}$$

- GW151226:

$$M_{\rm f}^{\rm source} = 20.8^{+6.1}_{-1.7}\,{\rm M}_\odot$$
$$a_{\rm f} = 0.74^{+0.06}_{-0.06}$$

- LVT151012:

$$M_{\rm f}^{\rm source} = 35^{+14}_{-4}\,{\rm M}_\odot$$
$$a_{\rm f} = 0.66^{+0.09}_{-0.10}$$

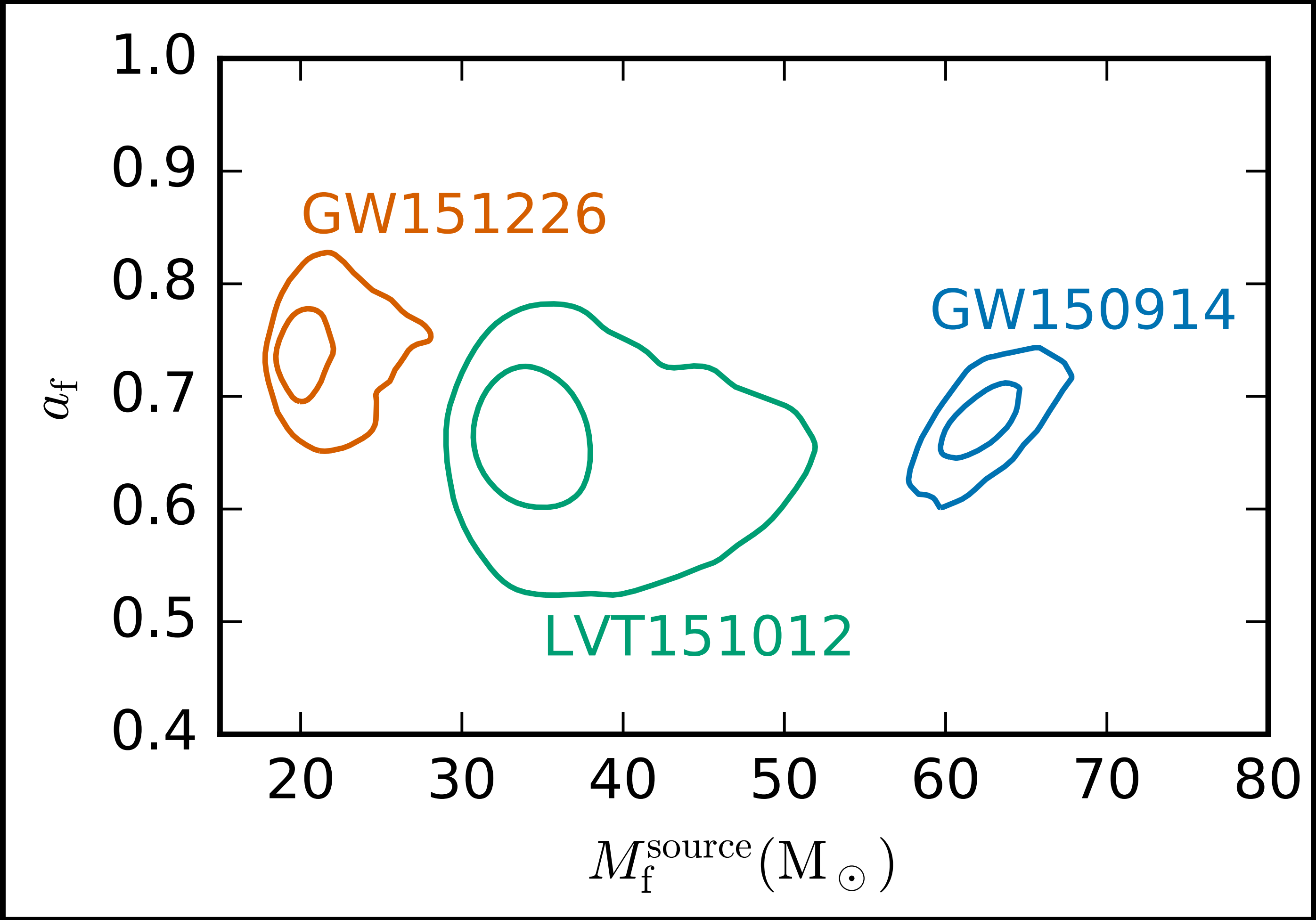

LSC+Virgo, arXiv:1606.04856

*Calculated using fitting formulae to NR. [17]

17. N.K. Johnson-McDaniel et al., Tech. Rep. LIGO-T1600168 (2016)

RADIATED ENERGY & LUMINOSITY

- GW150914:

$$E_{\rm rad} = 3.0^{+0.5}_{-0.4}\,{\rm M}_\odot c^2$$
$$\ell_{\rm peak} = 3.6^{+0.5}_{-0.4} \times 10^{56} {\rm erg/s}$$

- GW151226:

$$E_{\rm rad} = 1.0^{+0.1}_{-0.2}\,{\rm M}_\odot c^2$$
$$\ell_{\rm peak} = 3.3^{+0.8}_{-1.6} \times 10^{56} {\rm erg/s}$$

- LVT151012:

$$E_{\rm rad} = 1.5^{+0.3}_{-0.4}\,{\rm M}_\odot c^2$$
$$\ell_{\rm peak} = 3.1^{+0.8}_{-1.8} \times 10^{56} {\rm erg/s}$$

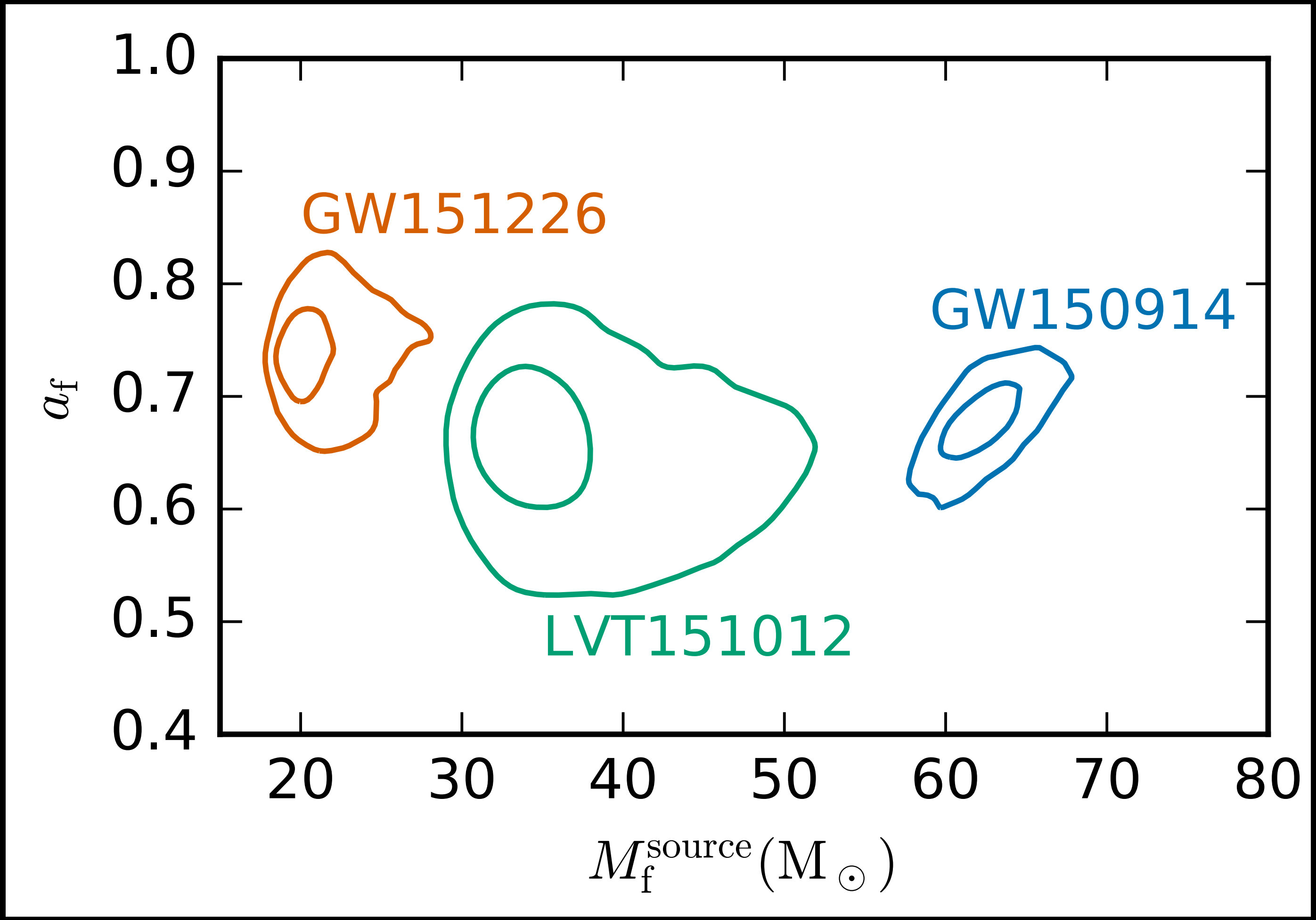

LSC+Virgo, arXiv:1606.04856

SKY LOCATION

- With 2 detectors can only limit location to annulus on the sky
- 90% credible regions:
- GW150914: 230 deg^2
- GW151226: 850 deg^2
- LVT151012: 1600 deg^2

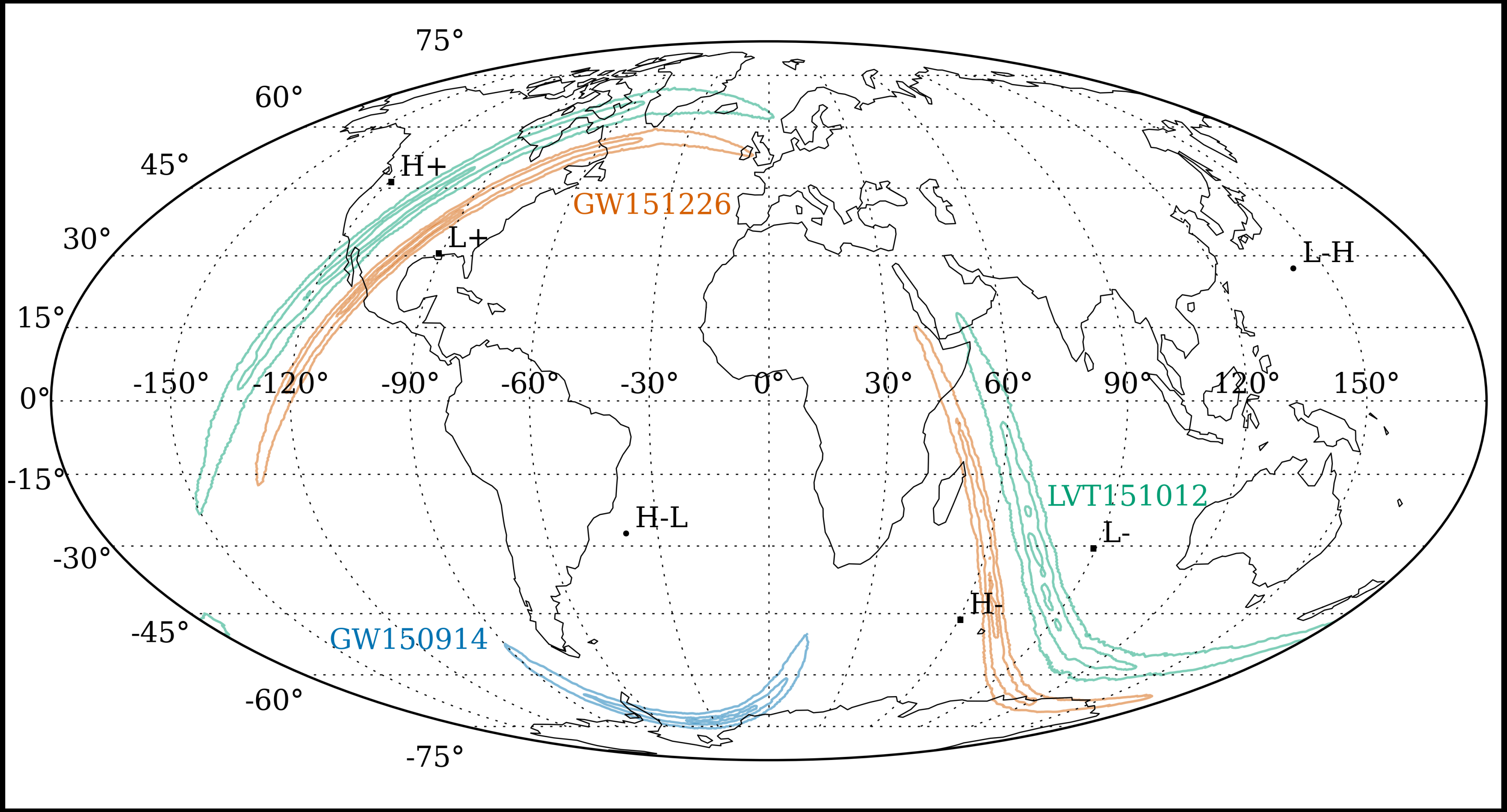

LSC+Virgo, arXiv:1606.04856

4. TESTS OF GR*

*See also talk by J. Meidam, C2

TESTS USING GW150914 [18]

- Inspiral/Merger-Ringdown consistency test
- Tests for the least damped QNM
- Constraints on parameterized deviations from GR waveforms
- Constraint on the graviton Compton wavelength
  - $\lambda_g < 10^{13}$kg [$m_g \leq 1.2 \times 10^{-22}$ eV/c^2]
- GR passed all tests

18. LSC+Virgo, PRL 116, 221101 (2016)

BANDWIDTH OF SIGNALS

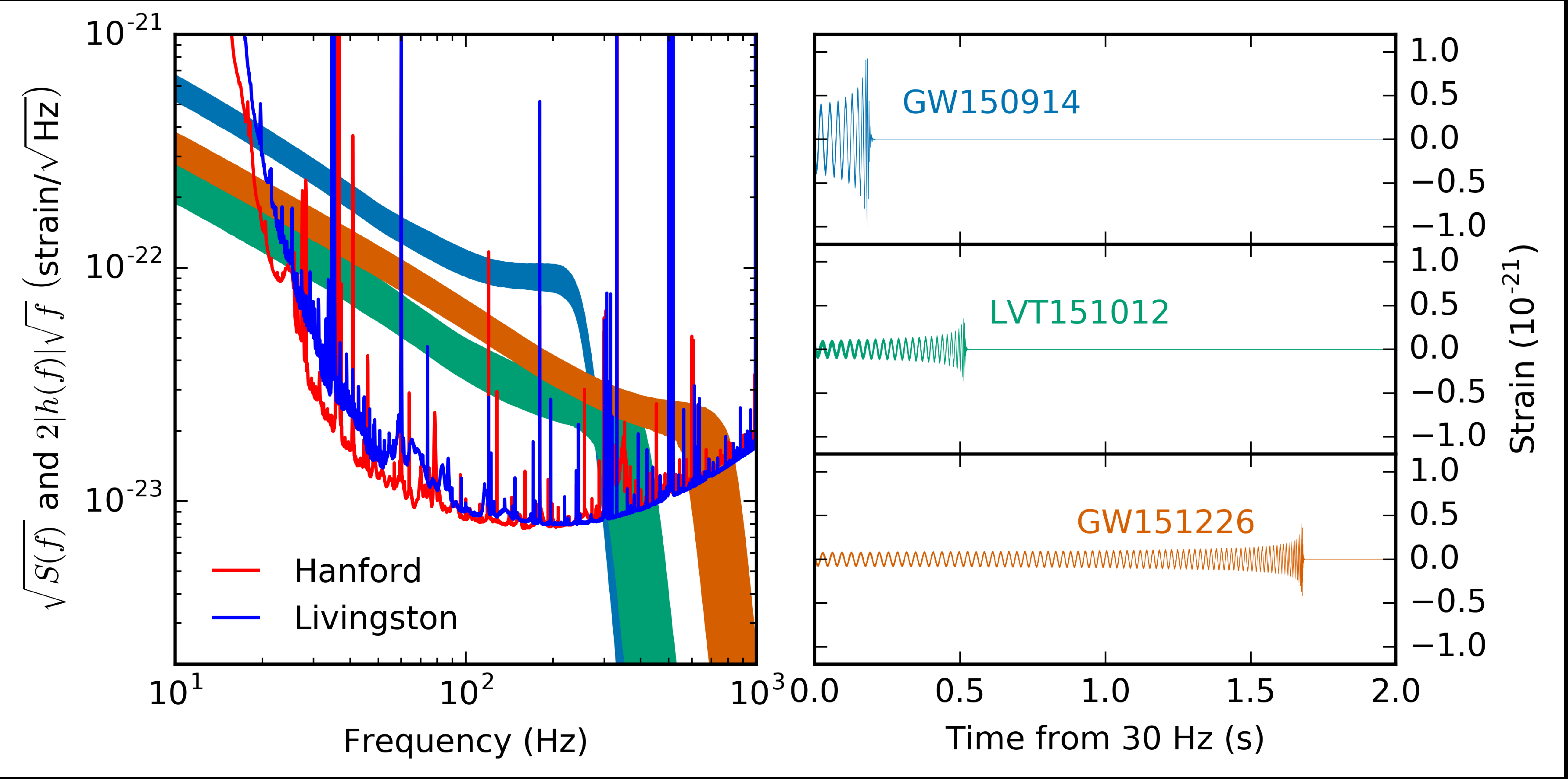

LSC+Virgo, arXiv:1606.04856

Tests using all events

- Inspiral/Merger-Ringdown consistency test
- Tests for the least damped QNM
- Constraints on parameterized deviations from GR waveforms
- Constraint on the graviton Compton wavelength

WAVEFORM PARAMETERIZATION

- IMRPhenom phase [19]:

$$\Phi_{\rm IMR} \sim \begin{cases} \frac{3}{128\eta} \sum_{j=0}^{7} \varphi_j(\Xi)(\pi M f)^{(j-5)/3} + \dots & f < f_1, \\ \frac{1}{\eta}\left(\dots + \beta_2 \log(f) - \frac{1}{3}\beta_3 f^{-3}\right) & f_1 \leq f < f_2, \\ \frac{1}{\eta}\left(\dots + \alpha_2 f^{-1} + \frac{4}{3}\alpha_3 f^{3/4} + \alpha_4 \tan^{-1}(af + b)\right) & f \geq f_2 \end{cases}$$

- Parameterize deviations to these coefficients [20]; e.g.:

$$\varphi_2'(\eta) = [1 + \delta\hat{\varphi}_2]\, \varphi_2(\eta)$$

- Vary deviations along with other parameters

19. S. Khan et al., PRD 93, 044007 (2016)
20. LSC+Virgo, PRL 116, 221101 (2016)

PARAMETERIZED TEST RESULTS

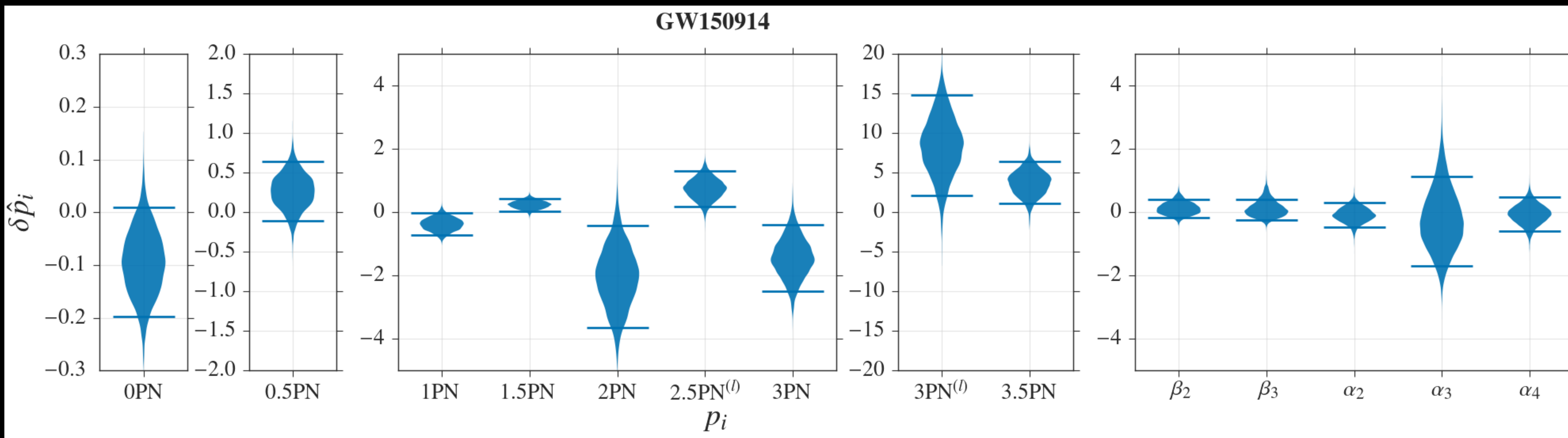

LSC+Virgo, arXiv:1606.04856

PARAMETERIZED TEST RESULTS

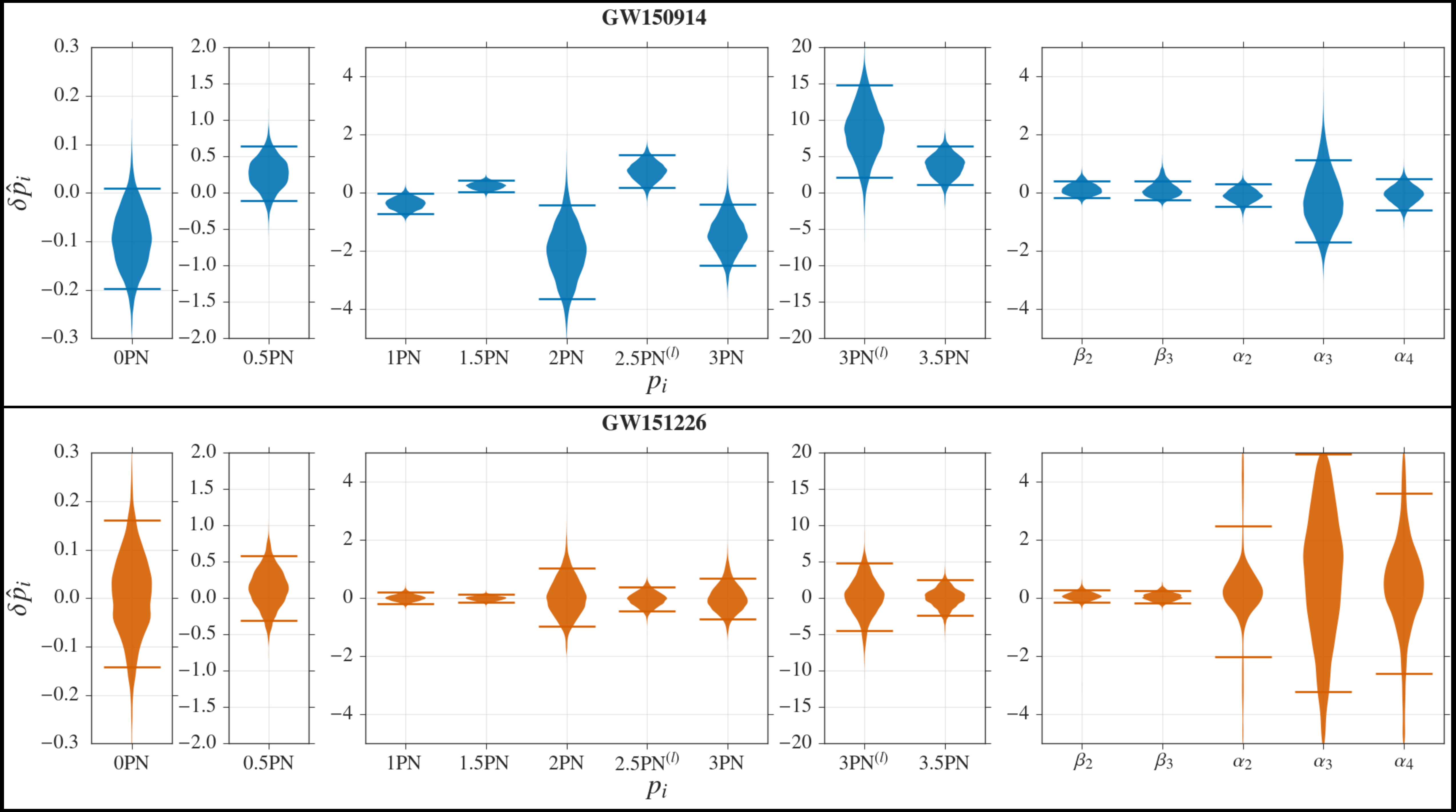

LSC+Virgo, arXiv:1606.04856

PARAMETERIZED TEST RESULTS

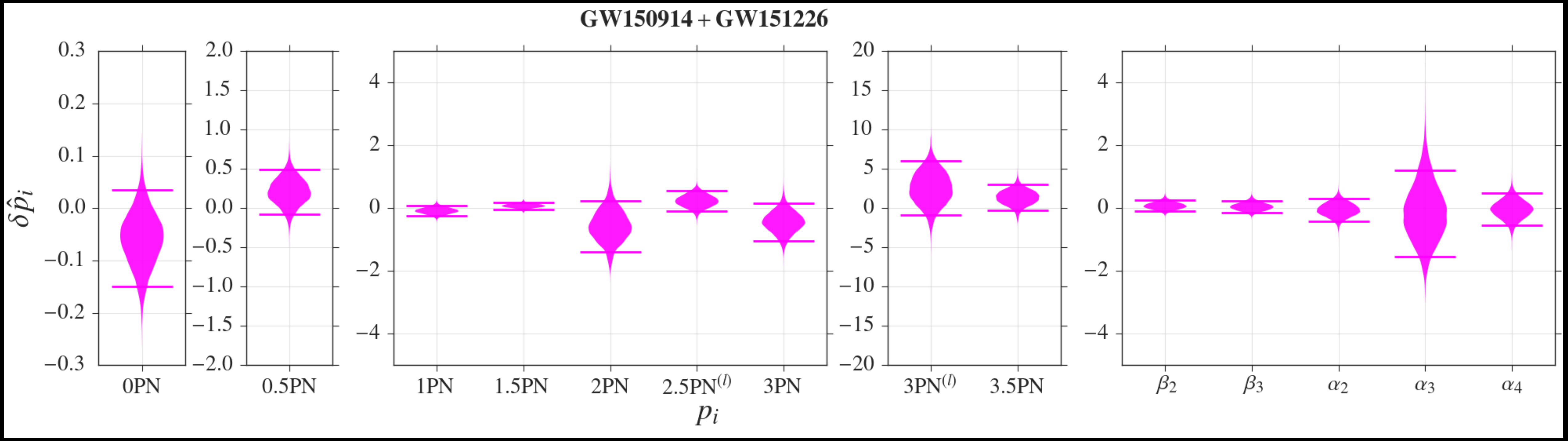

LSC+Virgo, arXiv:1606.04856

LOOKING FORWARD

- We estimate the rate of BBH coalescence
- GW150914+LVT151012:

  2 – 600 Gpc^{-3} yr^{-1} [18]
- +GW151226:

  9 – 240 Gpc^{-3} yr^{-1}
- See talk by T. Dent for details
- Estimate the probability of detecting N or more events in O2, O3

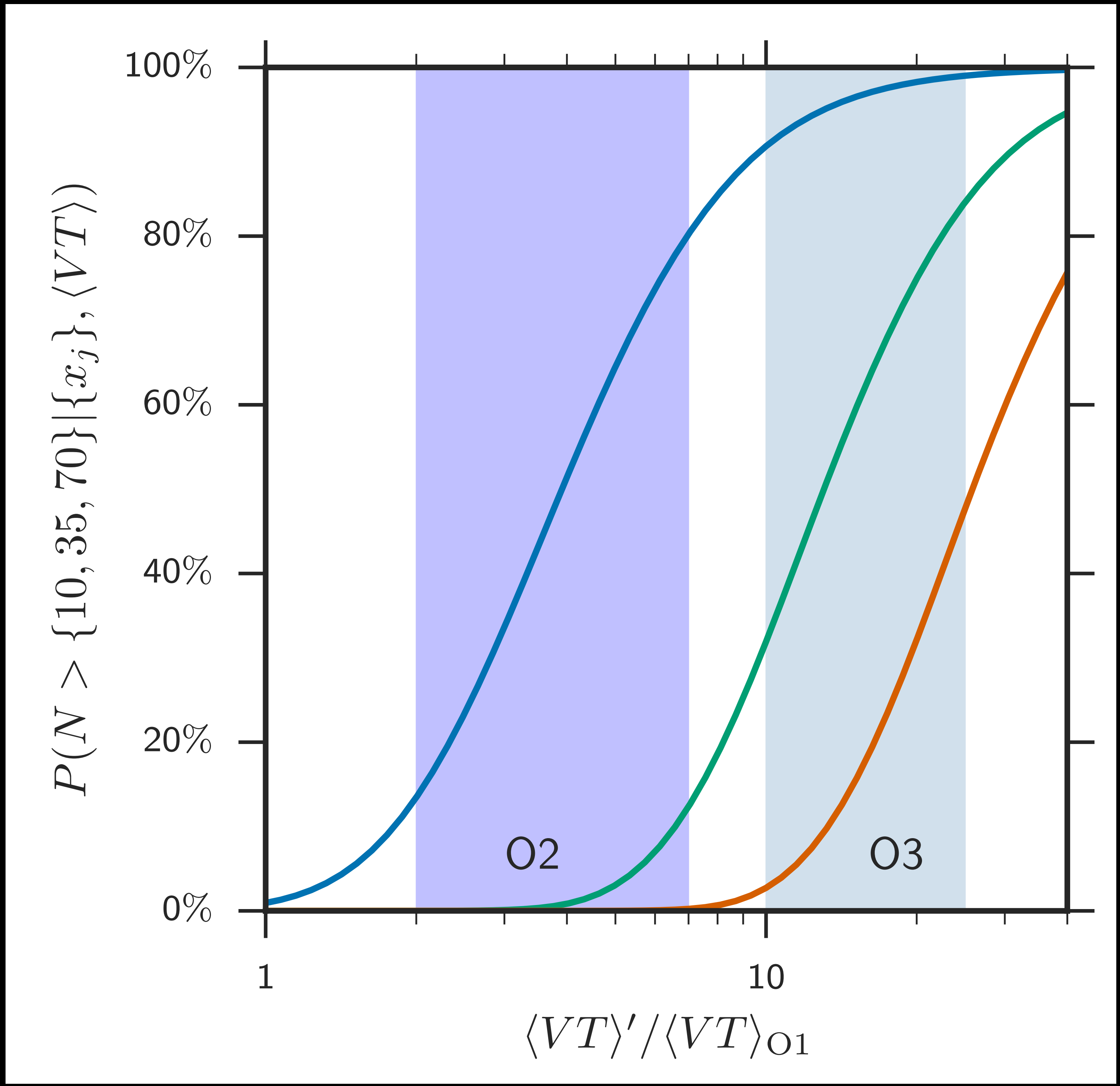

LSC+Virgo, arXiv:1606.04856

18. LSC+Virgo, arXiv:1602.03842

CONCLUSIONS

- We have confidently detected gravitational waves from 2 coalescing BBHs, GW150914 & GW151226, in O1.
- A third event, LVT151012, is also probably from a BBH.
- GW151226 has at least one component with spin ≥ 0.2
- All events are consistent with GR.
- O2 will bring more detections.
- The future is ~~bright~~ loud!

EXTRAS

	GW150914			GW151226			LVT151012		
	EOBNR	IMRPhenom	Overall	EOBNR	IMRPhenom	Overall	EOBNR	IMRPhenom	Overall
Detector frame									
Total mass $M/\mathrm{M}_\odot$	$71.0^{+4.6}_{-4.0}$	$71.2^{+3.5}_{-3.2}$	$71.1^{+4.1\pm0.7}_{-3.6\pm0.8}$	$23.6^{+8.0}_{-1.3}$	$23.8^{+5.1}_{-1.5}$	$23.7^{+6.5\pm2.2}_{-1.4\pm0.1}$	45^{+17}_{-4}	44^{+12}_{-3}	$44^{+16\pm5}_{-3\pm0}$
Chirp mass $\mathscr{M}/\mathrm{M}_\odot$	$30.4^{+2.3}_{-1.6}$	$30.7^{+1.5}_{-1.5}$	$30.6^{+1.9\pm0.3}_{-1.6\pm0.4}$	$9.71^{+0.08}_{-0.07}$	$9.72^{+0.06}_{-0.06}$	$9.72^{+0.07\pm0.01}_{-0.06\pm0.01}$	$18.1^{+1.3}_{-0.9}$	$18.1^{+0.8}_{-0.8}$	$18.1^{+1.0\pm0.5}_{-0.8\pm0.1}$
Primary mass $m_1/\mathrm{M}_\odot$	$40.2^{+5.2}_{-4.8}$	$38.5^{+5.4}_{-3.3}$	$39.4^{+5.4\pm1.3}_{-4.1\pm0.2}$	$15.3^{+10.8}_{-3.8}$	$15.8^{+7.2}_{-4.0}$	$15.6^{+9.0\pm2.6}_{-4.0\pm0.2}$	29^{+23}_{-8}	27^{+19}_{-6}	$28^{+21\pm5}_{-7\pm0}$
Secondary mass $m_2/\mathrm{M}_\odot$	$30.6^{+5.1}_{-4.2}$	$32.7^{+3.1}_{-4.9}$	$31.7^{+4.0\pm0.1}_{-4.9\pm1.2}$	$8.3^{+2.5}_{-2.9}$	$8.1^{+2.5}_{-2.1}$	$8.2^{+2.6\pm0.2}_{-2.5\pm0.5}$	15^{+5}_{-6}	16^{+4}_{-6}	$16^{+5\pm0}_{-6\pm1}$
Final mass $M_\mathrm{f}/\mathrm{M}_\odot$	$67.8^{+4.0}_{-3.6}$	$67.9^{+3.2}_{-2.9}$	$67.8^{+3.7\pm0.6}_{-3.3\pm0.7}$	$22.5^{+8.2}_{-1.4}$	$22.8^{+5.3}_{-1.6}$	$22.6^{+6.7\pm2.2}_{-1.5\pm0.1}$	43^{+17}_{-4}	42^{+13}_{-2}	$42^{+16\pm5}_{-3\pm0}$
Source frame									
Total mass $M^\mathrm{source}/\mathrm{M}_\odot$	$65.5^{+4.4}_{-3.9}$	$65.1^{+3.6}_{-3.1}$	$65.3^{+4.1\pm1.0}_{-3.4\pm0.3}$	$21.6^{+7.4}_{-1.6}$	$21.9^{+4.7}_{-1.7}$	$21.8^{+5.9\pm2.0}_{-1.7\pm0.1}$	38^{+15}_{-5}	37^{+11}_{-4}	$37^{+13\pm4}_{-4\pm0}$
Chirp mass $\mathscr{M}^\mathrm{source}/\mathrm{M}_\odot$	$28.1^{+2.1}_{-1.6}$	$28.1^{+1.6}_{-1.4}$	$28.1^{+1.8\pm0.4}_{-1.5\pm0.2}$	$8.87^{+0.35}_{-0.28}$	$8.90^{+0.31}_{-0.27}$	$8.88^{+0.33\pm0.01}_{-0.28\pm0.04}$	$15.2^{+1.5}_{-1.1}$	$15.0^{+1.3}_{-1.0}$	$15.1^{+1.4\pm0.3}_{-1.1\pm0.0}$
Primary mass $m_1^\mathrm{source}/\mathrm{M}_\odot$	$37.0^{+4.9}_{-4.4}$	$35.3^{+5.1}_{-3.1}$	$36.2^{+5.2\pm1.4}_{-3.8\pm0.4}$	$14.0^{+10.0}_{-3.5}$	$14.5^{+6.6}_{-3.7}$	$14.2^{+8.3\pm2.4}_{-3.7\pm0.2}$	24^{+19}_{-7}	23^{+16}_{-5}	$23^{+18\pm5}_{-6\pm0}$
Secondary mass $m_2^\mathrm{source}/\mathrm{M}_\odot$	$28.3^{+4.6}_{-3.9}$	$29.9^{+3.0}_{-4.5}$	$29.1^{+3.7\pm0.0}_{-4.4\pm0.9}$	$7.5^{+2.3}_{-2.6}$	$7.4^{+2.3}_{-2.0}$	$7.5^{+2.3\pm0.2}_{-2.3\pm0.4}$	13^{+4}_{-5}	14^{+4}_{-5}	$13^{+4\pm0}_{-5\pm0}$
Final mass $M_\mathrm{f}^\mathrm{source}/\mathrm{M}_\odot$	$62.5^{+3.9}_{-3.5}$	$62.1^{+3.3}_{-2.8}$	$62.3^{+3.7\pm0.9}_{-3.1\pm0.2}$	$20.6^{+7.6}_{-1.6}$	$20.9^{+4.8}_{-1.8}$	$20.8^{+6.1\pm2.0}_{-1.7\pm0.1}$	36^{+15}_{-4}	35^{+11}_{-3}	$35^{+14\pm4}_{-4\pm0}$
Energy radiated $E_\mathrm{rad}/(\mathrm{M}_\odot c^2)$	$2.98^{+0.55}_{-0.40}$	$3.02^{+0.36}_{-0.36}$	$3.00^{+0.47\pm0.13}_{-0.39\pm0.07}$	$1.02^{+0.09}_{-0.24}$	$0.99^{+0.11}_{-0.17}$	$1.00^{+0.10\pm0.01}_{-0.20\pm0.03}$	$1.48^{+0.39}_{-0.41}$	$1.51^{+0.29}_{-0.44}$	$1.50^{+0.33\pm0.05}_{-0.43\pm0.01}$
Mass ratio q	$0.77^{+0.20}_{-0.18}$	$0.85^{+0.13}_{-0.21}$	$0.81^{+0.17\pm0.02}_{-0.20\pm0.04}$	$0.54^{+0.40}_{-0.33}$	$0.51^{+0.39}_{-0.25}$	$0.52^{+0.40\pm0.03}_{-0.29\pm0.04}$	$0.53^{+0.42}_{-0.34}$	$0.60^{+0.35}_{-0.37}$	$0.57^{+0.38\pm0.01}_{-0.37\pm0.04}$
Effective inspiral spin χ_eff	$-0.08^{+0.17}_{-0.14}$	$-0.05^{+0.11}_{-0.12}$	$-0.06^{+0.14\pm0.02}_{-0.14\pm0.04}$	$0.21^{+0.24}_{-0.11}$	$0.22^{+0.15}_{-0.08}$	$0.21^{+0.20\pm0.07}_{-0.10\pm0.03}$	$0.06^{+0.31}_{-0.24}$	$0.01^{+0.26}_{-0.17}$	$0.03^{+0.31\pm0.08}_{-0.20\pm0.02}$
Primary spin magnitude a_1	$0.33^{+0.39}_{-0.29}$	$0.30^{+0.54}_{-0.27}$	$0.32^{+0.47\pm0.10}_{-0.29\pm0.01}$	$0.42^{+0.35}_{-0.37}$	$0.55^{+0.35}_{-0.42}$	$0.49^{+0.37\pm0.11}_{-0.42\pm0.07}$	$0.31^{+0.46}_{-0.27}$	$0.31^{+0.50}_{-0.28}$	$0.31^{+0.48\pm0.03}_{-0.28\pm0.00}$
Secondary spin magnitude a_2	$0.62^{+0.35}_{-0.54}$	$0.36^{+0.53}_{-0.33}$	$0.48^{+0.47\pm0.08}_{-0.43\pm0.03}$	$0.51^{+0.44}_{-0.46}$	$0.52^{+0.42}_{-0.47}$	$0.52^{+0.43\pm0.01}_{-0.47\pm0.00}$	$0.49^{+0.45}_{-0.44}$	$0.42^{+0.50}_{-0.38}$	$0.45^{+0.48\pm0.02}_{-0.41\pm0.01}$
Final spin a_f	$0.68^{+0.05}_{-0.07}$	$0.68^{+0.06}_{-0.05}$	$0.68^{+0.05\pm0.01}_{-0.06\pm0.02}$	$0.73^{+0.05}_{-0.06}$	$0.75^{+0.07}_{-0.05}$	$0.74^{+0.06\pm0.03}_{-0.06\pm0.03}$	$0.65^{+0.09}_{-0.10}$	$0.66^{+0.08}_{-0.10}$	$0.66^{+0.09\pm0.00}_{-0.10\pm0.02}$
Luminosity distance $D_\mathrm{L}/\mathrm{Mpc}$	400^{+160}_{-180}	440^{+140}_{-170}	$420^{+150\pm20}_{-180\pm40}$	450^{+180}_{-210}	440^{+170}_{-180}	$440^{+180\pm20}_{-190\pm10}$	1000^{+540}_{-490}	1030^{+480}_{-480}	$1020^{+500\pm20}_{-490\pm40}$
Source redshift z	$0.086^{+0.031}_{-0.036}$	$0.094^{+0.027}_{-0.034}$	$0.090^{+0.029\pm0.003}_{-0.036\pm0.008}$	$0.096^{+0.035}_{-0.042}$	$0.092^{+0.033}_{-0.037}$	$0.094^{+0.035\pm0.004}_{-0.039\pm0.001}$	$0.198^{+0.091}_{-0.092}$	$0.204^{+0.082}_{-0.088}$	$0.201^{+0.086\pm0.003}_{-0.091\pm0.008}$
Upper bound									
Primary spin magnitude a_1	0.62	0.73	0.67 ± 0.09	0.68	0.83	0.77 ± 0.12	0.64	0.69	0.67 ± 0.04
Secondary spin magnitude a_2	0.93	0.80	0.90 ± 0.12	0.90	0.89	0.90 ± 0.01	0.89	0.85	0.87 ± 0.04
Lower bound									
Mass ratio q	0.62	0.68	0.65 ± 0.05	0.25	0.30	0.28 ± 0.04	0.22	0.28	0.24 ± 0.05
Log Bayes factor $\ln\mathscr{B}_{s/n}$	287.7 ± 0.1	289.8 ± 0.3	—	59.5 ± 0.1	60.2 ± 0.2	—	22.8 ± 0.2	23.0 ± 0.1	—
Information criterion DIC	32977.2 ± 0.3	32973.1 ± 0.1	—	34296.4 ± 0.2	34295.1 ± 0.1	—	94695.8 ± 0.0	94692.9 ± 0.0	—

LSC+Virgo, arXiv:1606.04856

WAVEFORM MODELS

- "EOBNR": non-precessing spin model using effective-one-body (EOB) formalism tuned to numerical relativity (NR) (11 parameters) [13,14]
- "IMRPhenom": precessing waveform model derived from phenomenological fits of hybridized EOB & NR waveforms (13 parameters) [15,16]
- Precessing EOBNR used in later followup of GW150914 [17]
  - gives consistent results as IMRPhenom

13. A. Taracchini et al., PRD 89, 061502 (2014)
14. M. Pürrer, CQG 31, 195010 (2014)
15. M. Hannam et al., PRL 113, 151101 (2014)
16. P. Schmidt Ph.D. Thesis (2014)
17. LSC+Virgo, arXiv:1606.01210

GW150914 PE WITH PRECESSING EOBNR MODEL

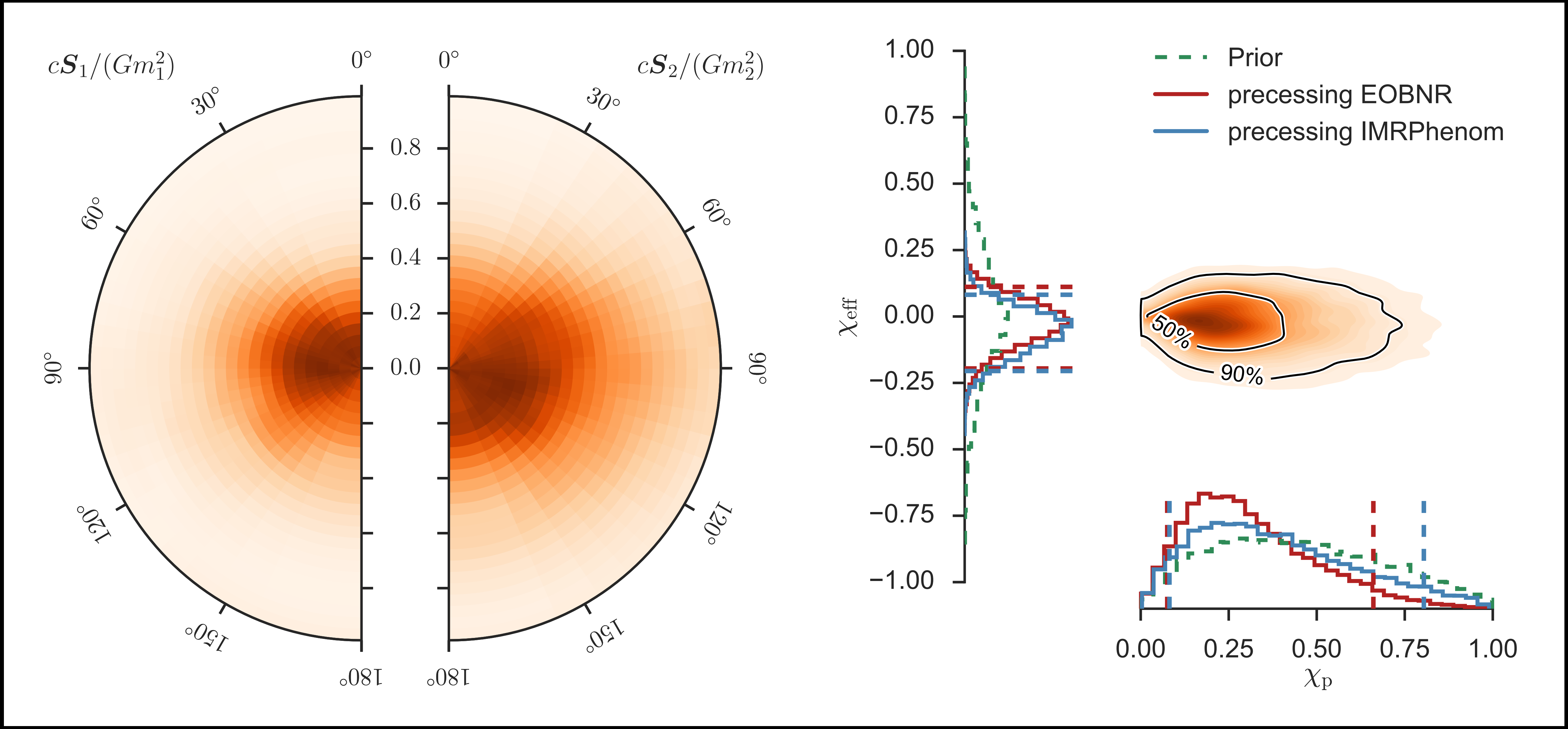

LSC+Virgo, arXiv:1606.01210

UNCORRELATED VS CORRELATED SOURCES

- FAR estimate gives rate of chance coincidences from uncorrelated noise sources
- Use environmental sensors to investigate any correlated noise sources
- No other environmental influences could be found [21]
- Conclude that GW150914 & GW151226 are gravitational waves.

21. LSC+Virgo, arXiv:1602.03844

Matched Filtering

- Have a signal buried in some strain s
- Use a template waveform h to calculate the signal-to-noise ratio (SNR) ρ:

$$\rho = \frac{|\langle h|s\rangle|}{\sqrt{\langle h|h\rangle}} \qquad \langle a|b\rangle \equiv 4\int_0^\infty \frac{\tilde{a}^*(f)\tilde{b}(f)}{S_n(f)}\mathrm{d}f$$

- By replacing h with $he^{-2\pi ift}$ we construct $\rho(t)$
- Triggers are points where $\rho(t)$ is maximized

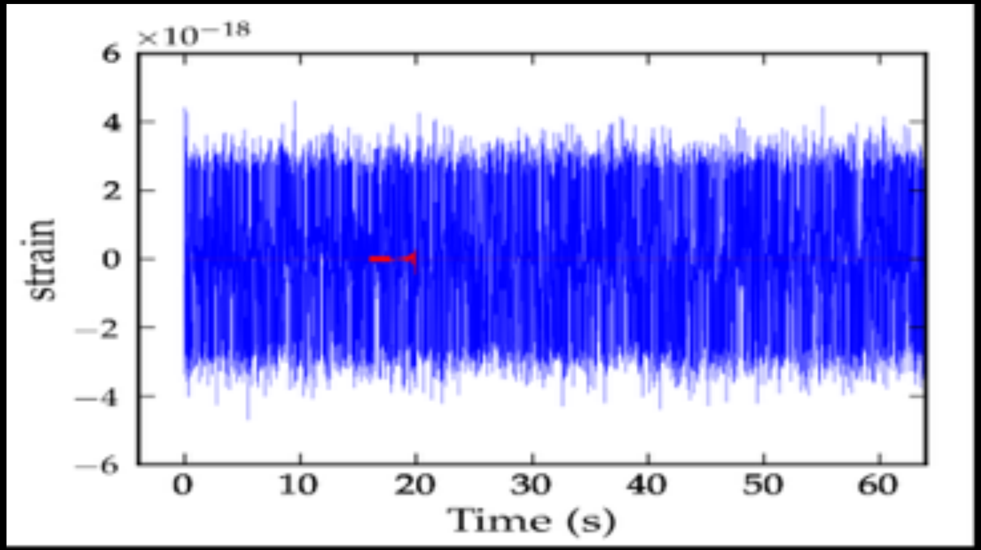

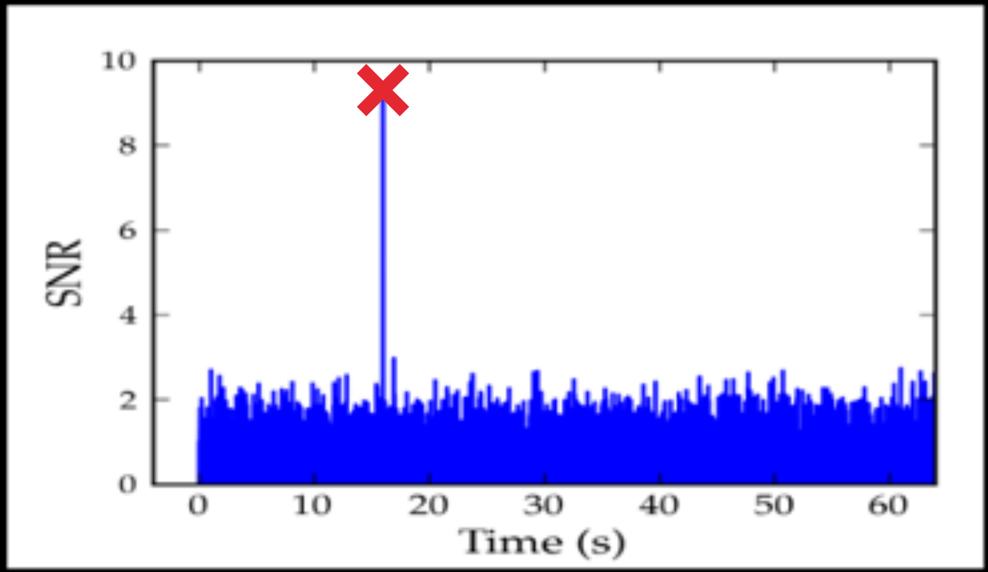

Courtesy A. Nitz

CBC PARAMETERS

- Possible CBC parameters (#):
  - component masses m_1, m_2 (2)
  - dimensionless spins of components χ_1, χ_2 (6)
  - location & orientation (6)

Precessing System

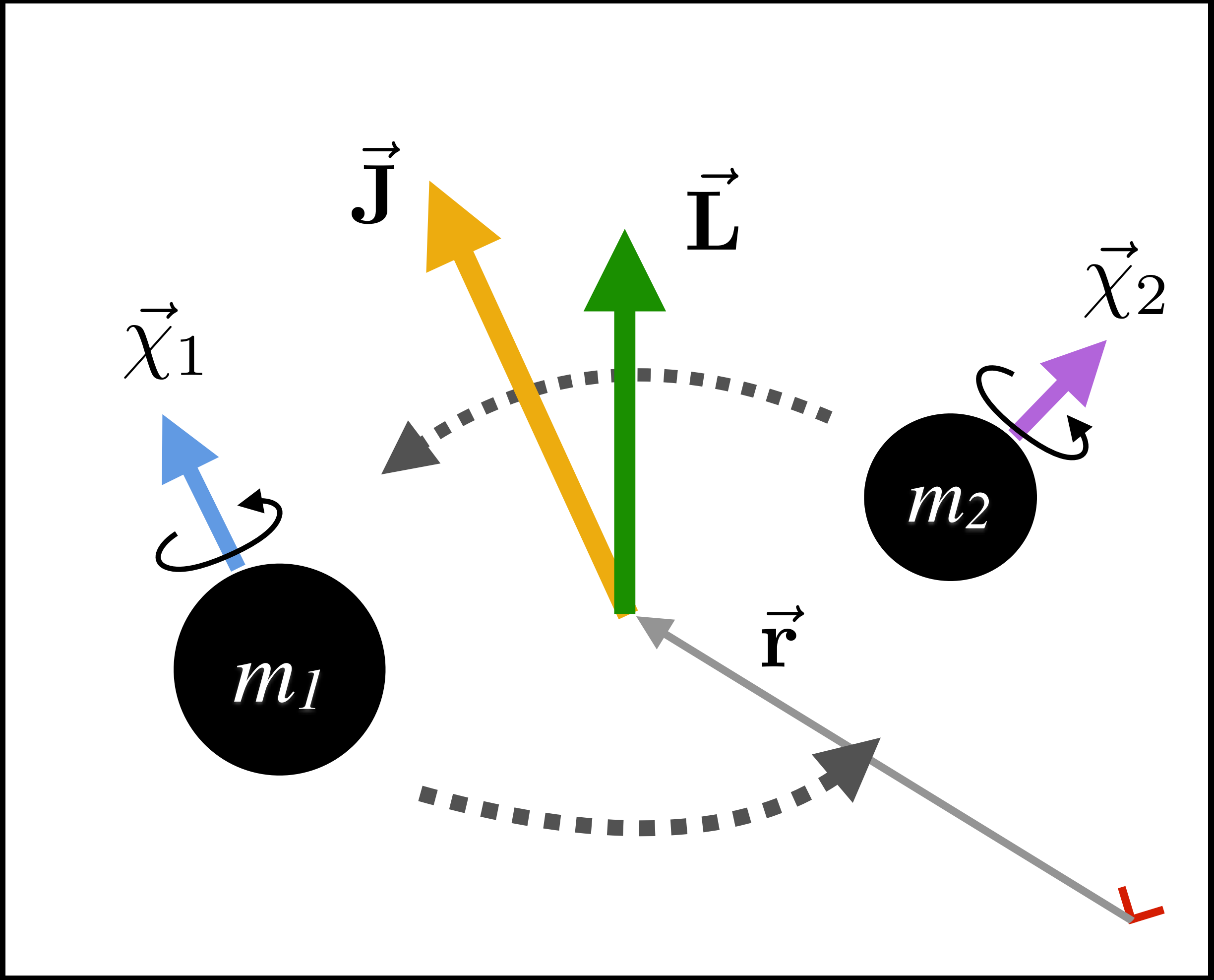

14 Parameters*

*not including coalescence time t_c, assuming circular orbit & 0 or negligible tidal deformation

CBC PARAMETERS

- Possible CBC parameters (#):
  - component masses m_1, m_2 (2)
  - dimensionless spins of components χ_1, χ_2 ~~(6)~~ (2)
  - ~~location & orientation (6)~~
    analytically maximized over for non-precession
- We consider non-precessing systems in our searches

Non-Precessing System

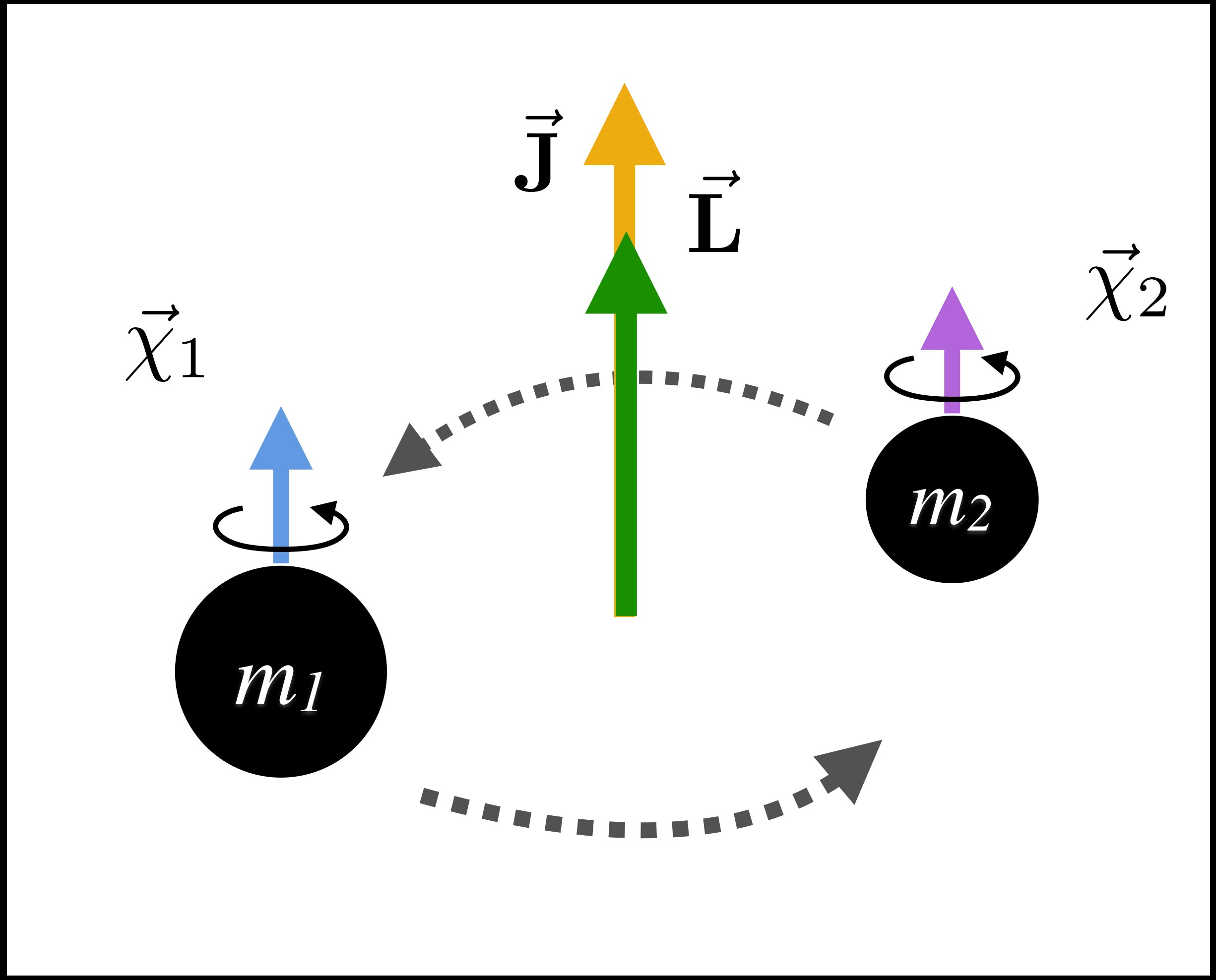

4 Parameters*

*not including coalescence time t_c, assuming circular orbit & 0 or negligible tidal deformation

COINCIDENCE TEST

- Apply a coincidence test to single-detector triggers
- Must be in same template & within ±15ms

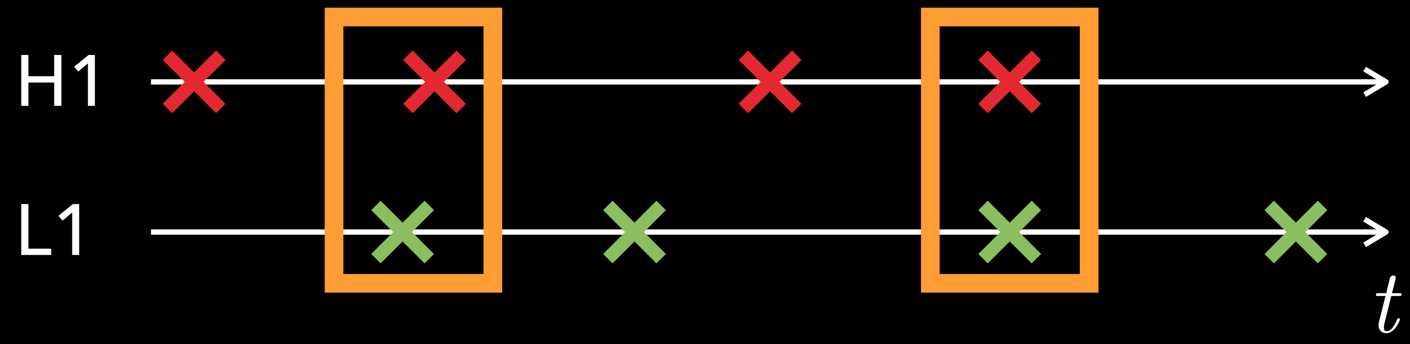

- Construct ranking statistic from reweighted SNR of coincident triggers:

$$\hat{\rho}_c = \sqrt{\hat{\rho}_H^2 + \hat{\rho}_L^2}$$

BACKGROUND ESTIMATE

- Do time slides to estimate background rate of false alarms

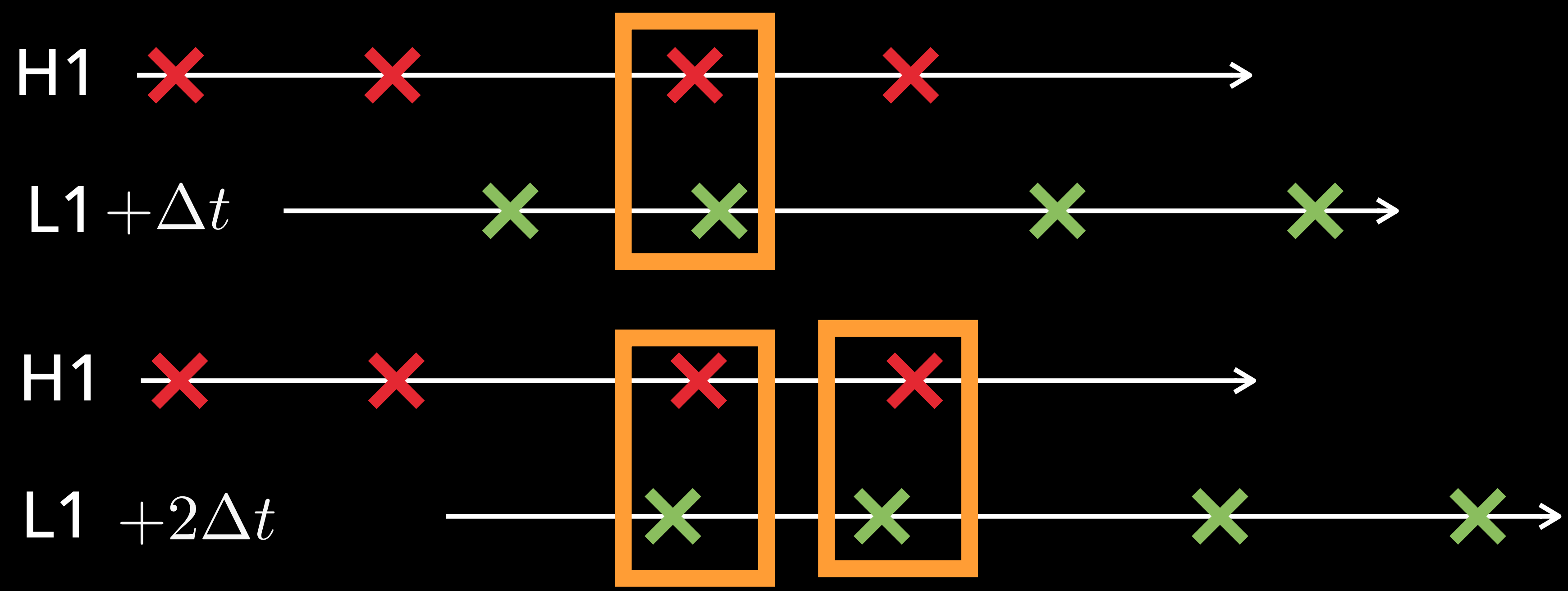

- Perform all possible Δt = 0.1s slides

$$\mathcal{F}(\hat{\rho}_c) \approx \frac{n_b(\hat{\rho}_c)}{N_S}; \quad \mathrm{FAR}(\hat{\rho}_c) \approx \frac{n_b(\hat{\rho}_c)}{N_S T}$$

PyCBC Chi-Squared Test

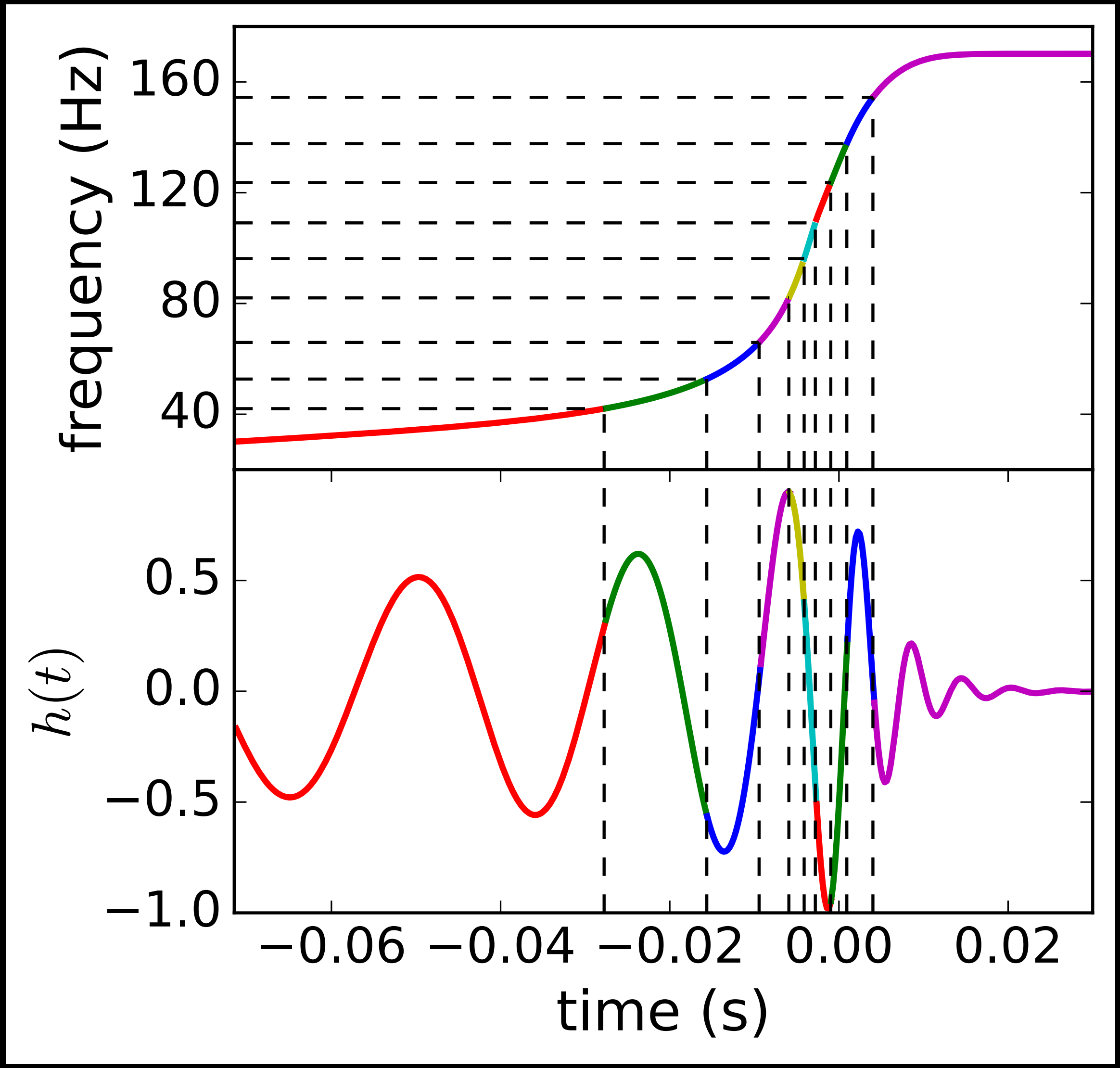

- Divide template h into p frequency bins of equal power
- Filter each h_i with the data s
- If template matches signal, expect:

$$\langle h_i | s \rangle = \langle h | s \rangle / p$$

- Calculate:

$$\chi_r^2 = \frac{p}{2p-2} \frac{1}{\langle h | h \rangle} \sum_{i=1}^{p} \left| \langle h_i | s \rangle - \frac{\langle h | s \rangle}{p} \right|^2$$

REWEIGHTED SNR

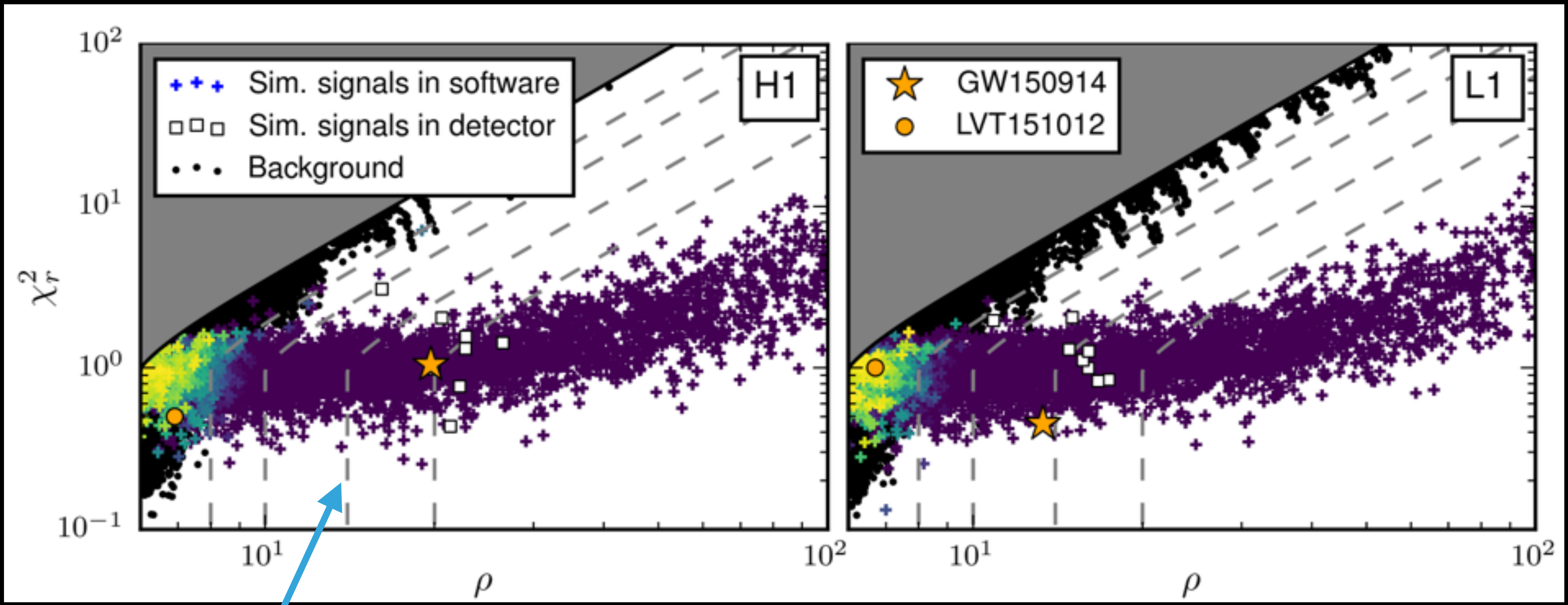

LSC+Virgo, PRD 93, 122003 (2016)

Reweighted SNR

$$\hat{\rho} = \begin{cases} \rho\left[(1+(\chi_r^2)^3)/2\right]^{-\frac{1}{6}}, & \text{if } \chi_r^2 > 1, \\ \rho, & \text{if } \chi_r^2 \leq 1. \end{cases}$$

Need for PE code

- Modeled searches are designed to identify times when a signal exists, estimate significance given non-Gaussian transients
- Discreteness of template bank ⇨ parameters of waveform not estimated accurately
- Need followup code

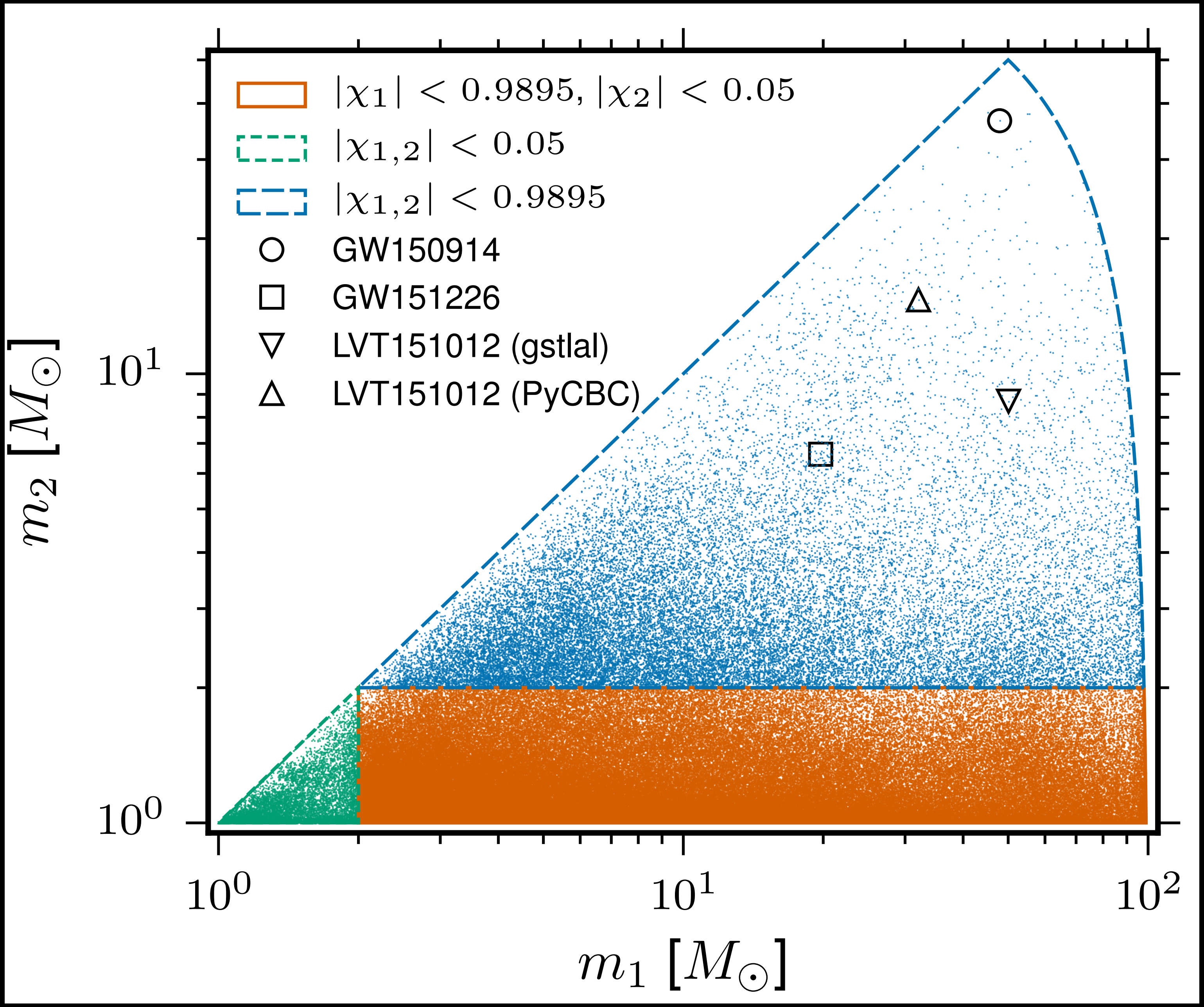

LSC+Virgo, arXiv:1606.04856

Bayes Theorem

- Probability that a waveform h with parameters $\vartheta = \{m_1, m_2, \ldots\}$ exists in data s is given by:

$$P(h[\vec{\vartheta}]|s) = \mathcal{L}(s|h[\vec{\vartheta}])P(h[\vec{\vartheta}]);$$
$$\mathcal{L}(s|h[\vec{\vartheta}]) = \text{``likelihood ratio''} \equiv \frac{P(s|h[\vartheta])}{P(s|0)}$$

- In N_d detectors with stationary Gaussian noise:

$$\mathcal{L}(s_k|h_k[\vec{\vartheta}]) \propto \exp\left[-\frac{1}{2}\sum_{k=1}^{N_d}\left\langle h_k[\vec{\vartheta}] - s_k \,\middle|\, h_k[\vec{\vartheta}] - s_k\right\rangle\right]$$

Matched-filter SNR = $\log\mathcal{L}$ maximized over phase & amplitude in single detector assuming non-precessing, dominant mode waveforms

INDEPENDENCE OF TIME SLIDES

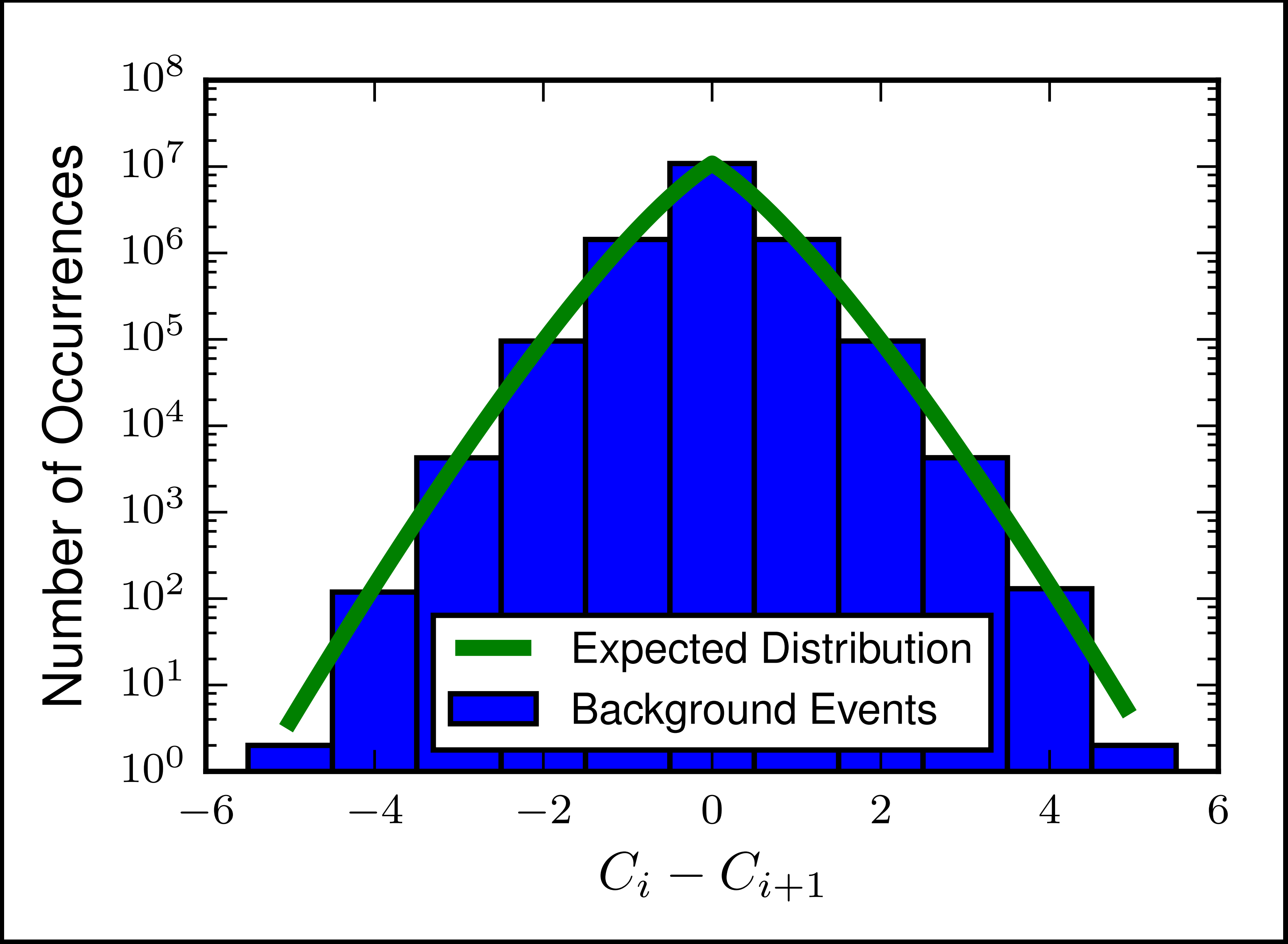

LSC+Virgo, PRD 93, 122003 (2016)